1970

Chemical interferences and ionization in high temperature flames

Donald Arthur Becker
Iowa State University

CHEMICAL INTERFERENCES AND IONIZATION IN HIGH TEMPERATURE FLAMES

by

Donald Arthur Becker

A Dissertation Submitted to the
Graduate Faculty in Partial Fulfillment of
The Requirements for the Degree of
DOCTOR OF PHILOSOPHY

Major Subject: Analytical Chemistry

Approved:

Signature was redacted for privacy.

In Charge of Major Work

Signature was redacted for privacy.

Head of Major Department

Signature was redacted for privacy.

Dean of Graduate College

Iowa State University
Of Science and Technology
Ames, Iowa

1970

TABLE OF CONTENTS

CHAPTER I. INTRODUCTION

The approach usually followed to introduce a dissertation on flame spectroscopy involves a historical development of flame photometric techniques and understanding. The historical development of flame applications is well documented in the literature (61, 92, 96): The first recorded observations, which bear any relation to flame photometry, date back to the middle of the 16th century. For approximately 200 years until the mid-1700's, several people described the coloration that certain salts imparted to simple flames. During the 1820's, Talbot and Herschel used flames for excitation sources and suggested a method of qualitative analysis based on the color emitted by various salts introduced into alcohol or candle flames. Kirchoff and Bunsen correlated spectral lines with specific elements in 1855, and in 1869 Janssen proposed a quantitative analysis technique based on a flame excitation source. Beginning in the late 1920's, Lundegardh set the basis for modern analytical flame spectrometry by developing flame systems as well as the entire spectroscopic apparatus. The basic works of Lundegardh, which are still valid today, established the starting point for the rapid development of improved techniques and equipment, which has continued throughout the world during the last forty years.

The preceding discussion merely establishes the fact that flames can serve as excitation sources. Nothing is mentioned concerning the present state of knowledge regarding the fundamental flame combustion processes. Thus, one is unmistakably led to believe that the combustion processes are trivial or too horribly complex to comprehend or discuss in a scientific manner.

Archaeological evidence suggests that fire was first used about 6×10^5 years ago (47), whereas fire was perhaps first created artificially about 3×10^4 years ago. The first scientific discussions regarding fire and flames were conducted by the Greeks around 400 B.C. In spite of the greatness of Alexander the Great, the early Greeks contributed virtually nothing to the understanding of combustion. So fire and flame remained as very mysterious phenomena, at least until 1852 when the following quotation appeared in Scientific American (41):

> ... It is our opinion that more discoveries will yet be made respecting flame and light....we are in the dark, yet, respecting one of the most common and simple chemical phenomena.

Following World War I, research centers supporting combustion research sprang up throughout the world. During the post World War II era, the United States Government supported combustion research through government contracts. However, the mystery of combustion is still not completely solved:

> ...Substantial progress has been made in establishing a common understanding of combustion phenomena. However, this progress of consolidation of the scientific approach to the subject is not yet complete. Much remains to be done to advance the phenomenological understanding of flame processes so that theoretical correlations and predictions can be made on the basis of secure and realistic models (B. Lewis and G. von Elbe, 1961 (88, p. v)).

> ...There has been a tendency in some groups--particularly among chemists interested in reaction kinetics--to dismiss flames as being too hopelessly complicated for fruitful study in any fundamental way. We believe, however, that research progress of the past ten or fifteen years has revealed the undue pessimism of this attitude and that the progress should be documented (R. M. Fristrom and A. A. Westenberg, 1965 (47, p. v)).

Future progress in combustion chemistry will perhaps be directed toward developing a rigorous flame theory consistent with detailed experimental studies. Admittedly, the very mechanism of flame propagation is at best fuzzy:

> ...When I first began the study of chemical kinetics, some forty-three years ago, the understanding of the mechanism of combustion reactions was in a very rudimentary state....it was clear that some general mechanism must be sought capable of giving a global explanation of this the oldest and longest studied chemical reaction....in particular, it is the conception of the branching-chain mechanism which provided the key to the problem, and which, since the middle 1920's, has proved both satisfying in clarifying our ideas, and fruitful in predicting new and profitable lines of experiment and research... the growth of the chain theory of combustion has followed ...(the line of seeking) to find the nature of the chain centers....the earlier chemical studies of combustion had led to the conclusion that reaction centers are usually to be identified with atoms and free radicals, and this view is still held....but it certainly proved difficult unequivocally to identify the centers and reactions involved....it is not my intention to enter into this rather weatherbeaten controversy (namely, the determination of reaction centers)....(R. G. W. Norrish, 1964 (101, p. 1)).

Although the combustion mechanism is not completely understood, flames need not be relegated to serve only as sources of life-sustaining heat energy. All enterprising spectroscopists realize that flames can serve as stable and reproducible excitation sources, and that flames are cheap to operate and simple to maintain. The behavior of analytical species introduced into flames can be studied in a fundamental manner in spite of the obvious uncertainty in the combustion mechanism.

CHAPTER II. CHEMICAL INTERFERENCES

Introduction

During the past ten years, simple combustion flames have become one of the most useful devices available to the analytical chemist for the quantitative determination of trace elements in solution. The usefulness stems from the very simple way that flames can release free atoms of various elements, which are found in solution. All that is necessary is to form an aerosol or spray from the solution and to introduce the spray into the flame. As the processes listed in Table 1 occur, a fraction of the dissolved sample is eventually converted into free atoms of the element being analyzed (analyte).

Table 1. Transformation of sample into atomic vapor

1. Nebulization of sample solution
2. Desolvation of wet aerosol
3. Volatilization of dry aerosol
4. Formation of molecular, atomic, and ionic species

Once the free atoms are formed, they can be detected at the trace level by three different spectroscopic techniques, namely, atomic absorption, atomic emission, and atomic fluorescence.

In flame photometric analysis, the relationship between the spectral emission or absorption intensity and concentration of the analyte is often equivocal. The published literature on flame emission and absorption spectroscopy contains many accounts concerning the influences certain constituents (interferents) in a sample may exert on the spectral signal of the analyte. These interelement effects are commonly referred to as interferences, which have been classified in accordance with their mechanism of origin (3; 52; 61, p. 61).

A satisfactory classification (52) of various types of interferences common to flame spectroscopy appears in Table 2.

Table 2. Classification of interferences

I. Spectral interferences
II. Physical interferences
III. Chemical interferences
A. Vapor-phase interferences
1. Excitation
2. Ionization
3. Dissociation
B. Condensed-phase interferences

Spectral interferences are realized when some flame species other than the analyte emits or absorbs radiation sufficiently close to the characteristic wavelength of the analyte. Generally, spectral interferences are more common in emission spectroscopy than in absorption spectroscopy. In the emission technique, the spectral region undergoing photometric detection is limited by the spectral bandpass of the monochromator. However, in absorption spectroscopy, a much narrower spectral region is observed when narrow line sources such as hollow cathode lamps serve as primary sources.

Physical interferences are non-specific in nature since the physical effects are generally limited to variations in the transport rate of the analyte into the flame. A potential non-specific interferent exercises the same relative effect on various elements and on varying concentrations of a single element. Physical interferents, which affect the physical properties of the sample solution, act to alter the process of aerosol formation either by reducing the quantity of aerosol or by changing the droplet-size distribution of the aerosol.

Chemical interferences include all reactions that are specifically dependent on the chemical nature of the analyte. Chemical interferences may occur with the vapor-phase or condensed-phase forms of the analyte.

Excitation interferences are not common in flame spectroscopy since most flames are in thermal equilibrium beyond the primary reaction zone. However, if a combustible solvent replaces an aqueous solvent in the sample solution, the flame temperature will change and an excitation interference will occur. Excitation interferences generally merit more consideration in emission spectroscopy than in absorption spectroscopy.

Ionization interferences are chemically specific mainly because of the variation of ionization energies among the elements. For an ionization interference to occur, the analyte must be appreciably ionized in the flame. Elements capable of being ionized in conventional flames are generally limited to the alkali, alkaline earth, and rare earth groups of metals. An ionization interferent is some species capable of altering the free-electron density in the flame, thereby shifting the ionization-recombination balance of the atomic and ionic forms of the analyte.

Dissociation interferences are similar to ionization interferences in that a shift in a chemical balance is involved. A dissociation interference results when an interferent changes the relative amounts of an analyte present as atomic and molecular vapor. Dissociation reactions are also specific since the relative amounts of molecular and atomic analyte depend on the chemical nature of the analyte.

The condensed-phase or solute-vaporization chemical interference is perhaps the most troublesome chemical interference. Historically, many journal articles have described solute-vaporization interferences associated with flame spectroscopic techniques (52, 61). A condensed-phase interferent is one that inhibits the vaporization of the desolvated aerosol droplet containing the analyte. The exact mechanisms by which solute-vaporization interferences occur are not known although many explanations have been proposed to account for the interference effect. The published accounts of many solute-vaporization interferences are often inconsistent with one another in relating the magnitude and the direction of the interference; this implies the observed interference also includes physical effects dependent on the experimental apparatus. The interference investigation described herein was initiated in order to find some simple and convenient means of eliminating several common condensed-phase interferences.

The nature of condensed-phase chemical interferences

The literature contains excellent reviews on the nature of condensed-phase interferences (3; 8; 61, p. 300; 113); several points regarding their interpretation have found general acceptance among analytical flame spectroscopists. The most common condensed-phase chemical interference systems include the effect of phosphate, sulfate, and aluminum on the

emission and absorption signals of the alkaline earth metals. If, for example, the calcium-phosphate interference is studied in either a low temperature flame stabilized by an indirect nebulizer-burner[1] or a flame stabilized by an integral nebulizer-burner, the literature quite typically describes the interference in the following way (8, 12, 34, 35, 48,89, 91, 132, 137): The depression in the emission or absorption intensity of calcium as a function of increasing phosphate is usually reported as being linear up to phosphate/Ca ratios of approximately one. Near molar ratios of one, a bend occurs in the interference curve and the analytical signal is not sensitive to increasing amounts of interferent beyond the bend.

In attempts to interpret the experimental calcium-phosphate interference curves, a number of investigators hypothesized that the decrease in intensity resulted because calcium and phosphate formed a refractory compound whose greater thermal stability limited the release of free calcium atoms. Credence is given to this interpretation by the observation that no calcium emission intensity suppression occurred when an

---

[1]An indirect nebulizer-burner possesses an intermediate spray chamber between the nebulizer and the flame. A direct or integral nebulizer-burner is a single unit that sends the entire aerosol directly into the flame without passage through any intermediate channels between the nebulizer and the burner port.

interferent-free calcium solution and a solution of phosphoric acid were nebulized separately but simultaneously and then introduced into the flame (7, 48, 111). Phenomenologically, the interference mechanism may be outlined as follows (61, p. 304): During the dehydration of the aerosol droplet, the calcium has every opportunity to react with phosphorus at the combining ratio to form a refractory compound, e.g., $Ca_2P_2O_7$ or $Ca_3(PO_4)_2$. The bend in the interference curve may then be interpreted as the chemical combining ratio of the calcium and phosphorous in the refractory species. Any excess phosphorous beyond the point indicated by the bend evidently vaporizes quite rapidly and no further interference results.

The alkaline earth-aluminum interference systems have shared the popularity spotlight with the phosphate interference systems. The aluminum interferences, which have also been classified as condensed-phase interferences, react to the separate nebulization experiments in the same manner as the phosphate interferences (7, 48). The magnitude and persistence of the alkaline earth-aluminum interferences in relatively low temperature flames or flames provided by direct nebulizer-burners are aptly illustrated in the literature (8; 48; 61, p. 303; 91).

Although the alkaline earth-aluminum interference curves do not generally indicate the sharp bend, which is characteristic of the phosphate interference, the postulated mechanism of

interference also involves the production of an involatile compound between the analyte and interferent (e.g., $CaAl_2O_4$) (91, 117). Another possible cause for the observed interference is the occlusion of the analyte in a stable matrix of the interferent (3).

The reduction and elimination of condensed-phase chemical interference effects

The acknowledgement of condensed-phase chemical interferences did not severely limit the range of application of flame spectroscopic techniques. The major effects of these interferences were manifested as gross inconveniences. Herrmann et al. (61, p. 320) list nearly twenty procedural methods for reducing (and sometimes eliminating) chemical interferences. These methods range from separation of the analyte from the interferent to the preparation of standards, which simulate the interference system. Certain additives (compounds added to the sample solution) have been used with some apparent success to provide a means for coping with condensed-phase chemical interferences. Buffering additives essentially act to dominate the interference, thereby saturating the interference effects (52). Releasers and protectors act to remove the interference by preventing the formation of an involatile analyte-interferent complex (52). Releasers have been used quite successfully (26, 27, 33, 137), and a mechanism describing their action has been suggested

(33). Protectors have been used with limited success (133), and their mechanism of action is equivocal (11). However, protectors supposedly act directly on the analyte, thereby preventing direct interactions between the analyte and interferent (52, 134).

One is not of necessity restricted to the addition of additives, the preparation of simulated standards, or prior chemical separations when attempting to cope with chemical interferences. Often these methods are inconvenient and inadequate for accurate analytical flame spectroscopy. Other factors that facilitate the production of free atoms in flames can be optimized to minimize or eliminate chemical interferences.

The effect of aerosol droplet-size The genesis of free atoms in a flame must proceed through the various steps listed in Table 1; some of the processes noted therein may occur simultaneously. The steps listed in Table 1 involve physical processes such as nebulization and desolvation, which may indirectly contribute to a condensed-phase chemical interference. For example, solute-vaporization interferences are notably more severe when integral nebulizer-burners of the Beckman type (61, p. 122) rather than indirect nebulizer-burners are employed as part of the spectroscopic apparatus (61, p. 301). Several reasons account for this observation. The Beckman integral aspirator produces an aerosol whose mean

droplet-size (28) is significantly larger than the mean droplet-size of the aerosol emanating from an indirect nebulizer-burner (135). Since the time required for desolvation is proportional to the square of the mean drop size (6; 28; 61, p. 24), evaporation of the solvent requires more time when integral nebulizer-burners of the Beckman type are employed. Large wet aerosol particles reaching the flame will necessarily lead to large dry aerosol particles. The time required to vaporize a solute particle is also proportional to the square of the mean particle size (6, 11). If the solute particle is relatively stable with respect to the volatilization process, condensed-phase chemical interferences will appear to be more severe for larger aerosol droplets. Therefore, the production of free atoms in flames may be enhanced by an efficient nebulization process.

The effect of organic solvents The enhancements in absorption or emission signals afforded through the use of organic solvents for the sample solution, or the addition of organic components to the solution, have been adequately documented (61, p. 22). Systematic studies on the mechanism of this enhancement effect have clearly shown that the gain in signals depends in a rather complicated and subtle way on the combined action of many factors. Clearly, several of the factors, which contribute to spectral enhancements, should at the same time lead to a minimization or elimination of

condensed-phase chemical interferences. In particular, the presence of organic components with surface tensions lower than that of H_2O either as solvents or additions to the solution, should lead to the formation of a finer spray by the process of pneumatic nebulization (28; 61, p.22). If the vapor pressure of the organic component is at the same time greater than that of water, and is combustible as well, the increase in the evaporation constant (60) should contribute to a marked increase in the overall efficiency of vaporization of the aerosol droplet and its residue.

The effect of flame temperature Another factor, which notably affects the rate of solute vaporization, is the temperature of the flame. The time required for complete volatilization is a direct function of the absolute flame temperature (6, 11). The importance of the temperature factor in reducing the magnitude of condensed-phase chemical interferences has been demonstrated (61, p. 74, 308).

The experimental approach The importance of flame temperature and refinement of the sample aerosol in reducing the magnitude of solute-vaporization interferences points out that there is often not enough time for the aerosol particle to vaporize completely during its transit through the flame. For example, condensed-phase chemical interferences are found to be greatly diminished in magnitude when the spectral signal of the analyte is sampled at greater observation heights in

the flame (8, 48).

Recent developments in burner design and high temperature premixed flame systems have provided the analyst with opportunities to exercise a higher degree of optimization of the variables known to reduce the severity of condensed-phase chemical interferences. It is somewhat surprising that little effort has been devoted to taking advantage of these developments in directly eliminating all vestiges of several important chemical interferences, without resorting to the addition of extraneous releasers, protectors, or buffers or resorting to prior chemical separations. The data to be presented will show that the depressant effects exerted by the classical chemical interferents on the emission and absorption signals of alkaline earth metals can be eliminated at interferent concentrations normally encountered by taking advantage of the flame systems and the optimal nebulization characteristics of the nebulizer-burners systems described below.

Experimental Facilities and Procedures

Two different nebulizer-burner systems were employed for the majority of the investigations of several common condensed-phase chemical interferences. One of these was the premixed O_2-N_2-C_2H_2 burner[1] (see Figure 1) previously described by D'Silva, Kniseley, and Fassel (39). A second nebulizer-burner used herein was the long-path slot burner presented in Figure 2 (46). In operation, each of these burners refines the nebulized aerosol so that a smaller drop-size distribution is introduced into the flame. In the premixed O_2-N_2-C_2H_2 burner, the premixing channel (the hypodermic tubing) in effect serves as an extended impact plate and as a spray chamber to lower the drop-size distribution formed by the Beckman nebulizer-burner.

An unmodified integral Beckman burner (in Figure 1, the premix burner without the premixing chimney) was also used for one brief experimental study.

---

[1]Premixed burner refers to a burner in which the combustion gases are premixed prior to ignition.

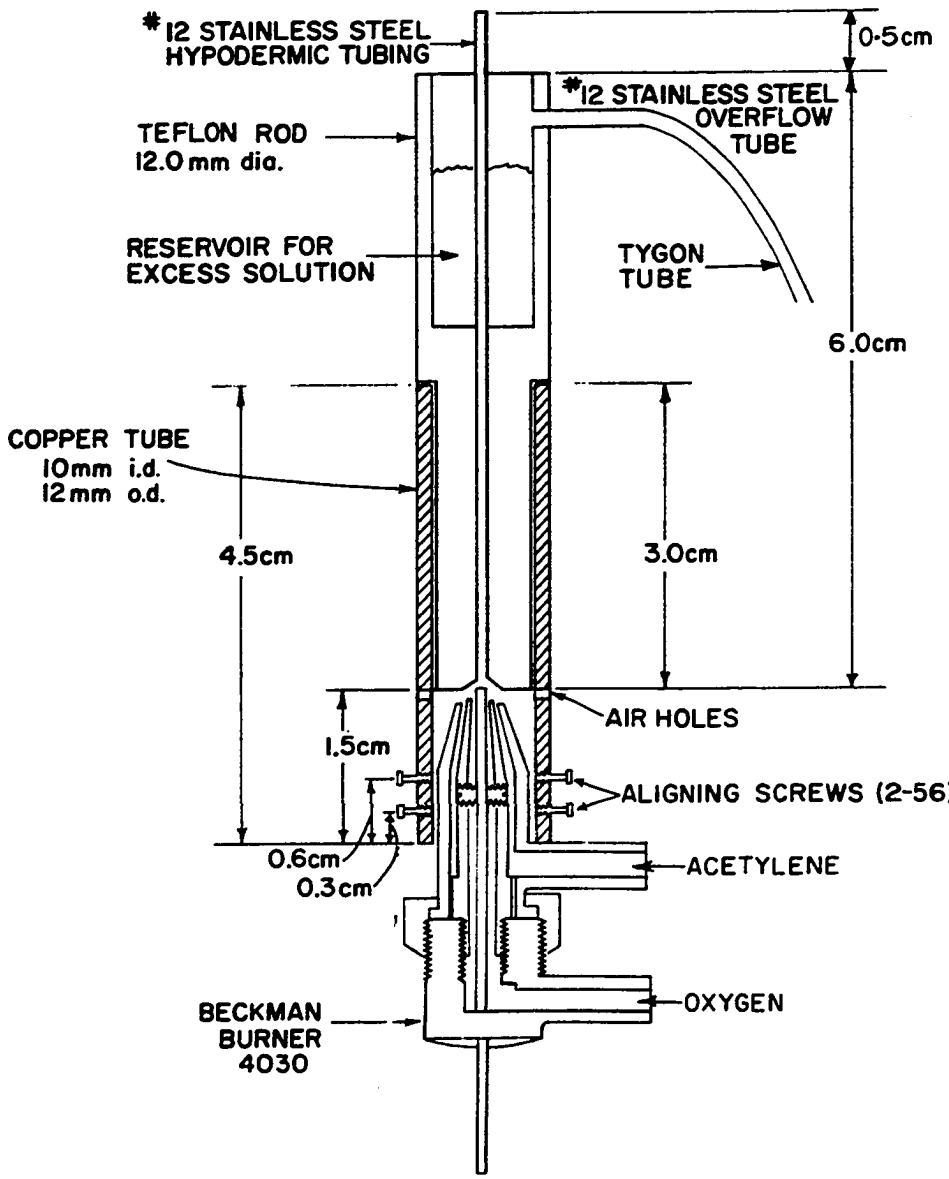

Figure 1. Cross-sectional drawing of the premixed oxygen-nitrogen-acetylene burner

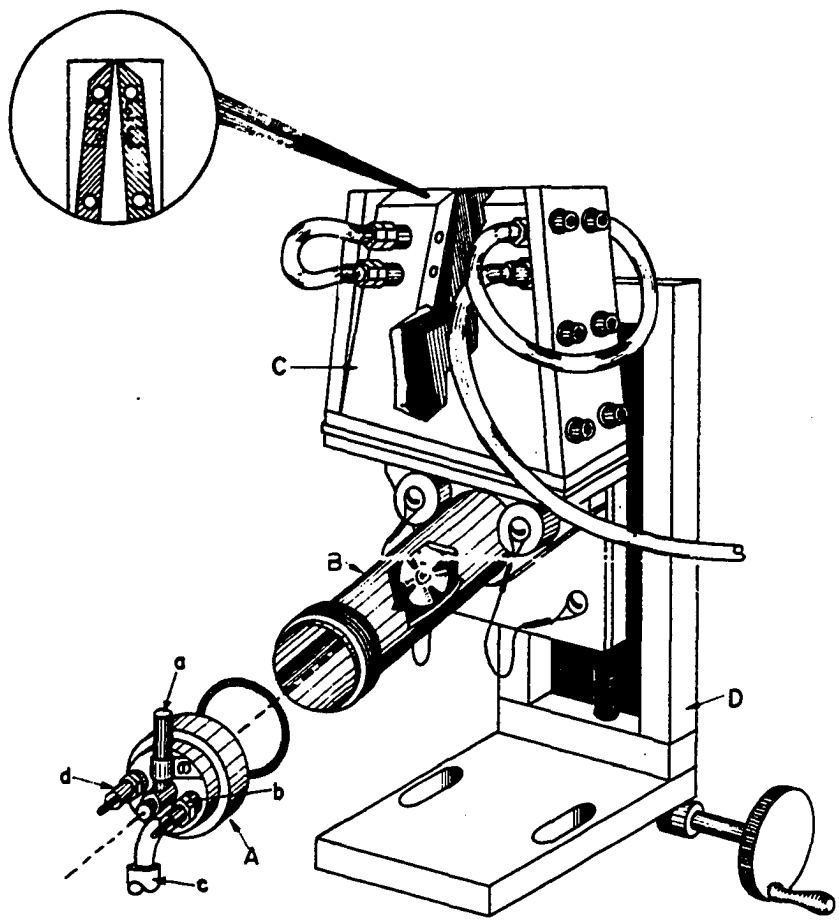

(A) End-cap assembly showing (a) nebulizer; (b) and (d) fuel port and auxiliary oxidant port; (c) drain pipe
(B) Spray-premixing chamber showing flow spoiler and blow-out plugs
(C) Burner head showing tapered walls and cooling ducts
(D) Burner racking assembly

Figure 2. Cutaway view of long-path slot burner

Flame temperatures and pertinent data regarding the gas flow rates employed with the respective burner systems are listed in Table 3.

Table 3. Burner operating conditions and flame temperatures

Burner	Gases and flow rates[a] l /min		Temperature[a] at 20 mm °K	
Beckman burner (61, p. 122)	O_2	3.2	~ 3000	(99)
	C_2H_2	2.1		
Premixed O_2-N_2-C_2H_2 burner (39)	O_2	3.8	~ 2700	(99)
	C_2H_2	4.8		
Slot burner (46)	N_2O	11.3	~ 2800	(136)
	C_2H_2	6.4		
Slot burner (46)	O_2	13.7	~ 2950[b]	
	C_2H_2	14.2		

[a]These gas flow rates and corresponding flame temperatures where characteristic of the flames used for analyzing solutions whose solvent was 50% EtOH-50% H_2O. When aqueous solutions were sampled, the acetylene flow rates for the N_2O-C_2H_2 and O_2-C_2H_2 slot burner flames were increased to 7.4 (Temp. = 2880 °K[b]) and 15.0 (Temp. = 3000 °K[b]) l/min, respectively.

[b]These are measured line reversal temperatures. The principle of the line reversal technique is discussed in Chapter III.

Along with a burner and flame support system, the spectroscopic apparatus must include some device for wavelength selection, a detector, and readout devices. Block diagrams listing the components used for performing atomic emission and absorption experiments are presented in Figures 3 and 4. Details of the individual components are listed in Table 4.

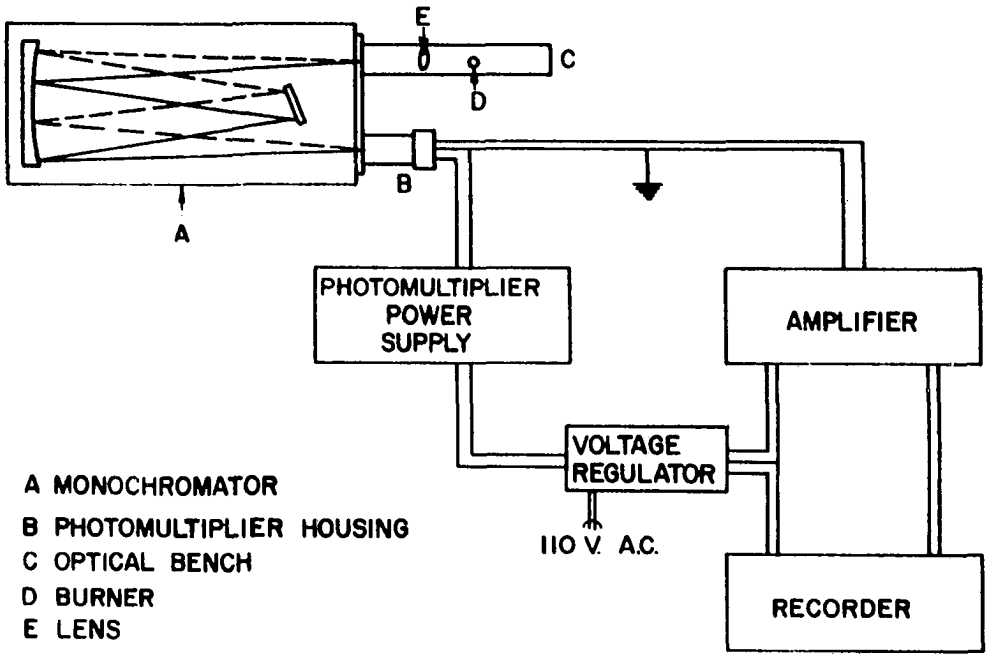

Figure 3. Block diagram of emission system

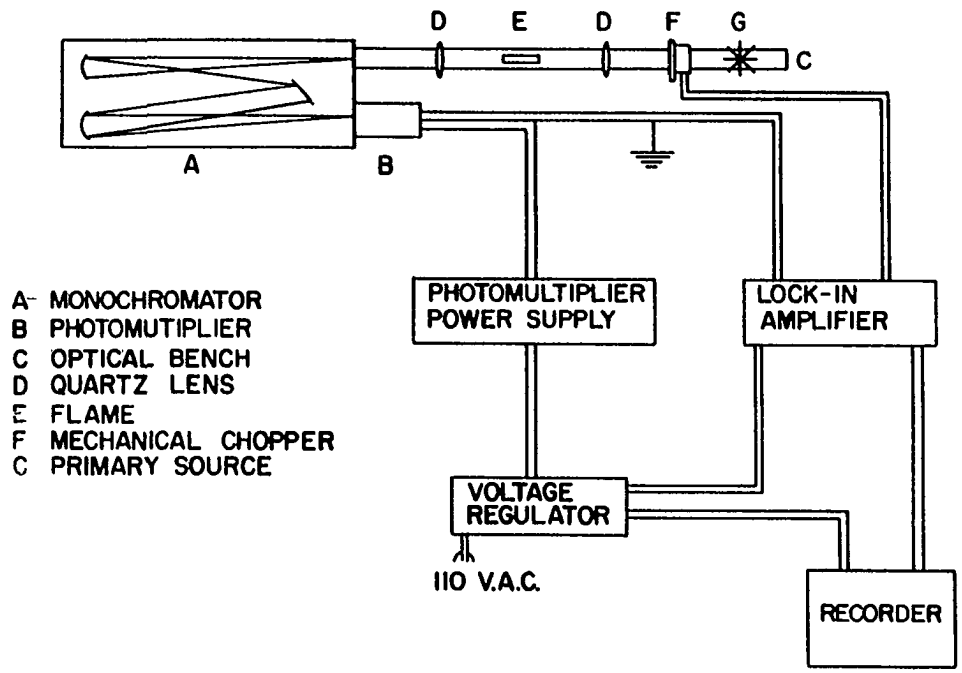

Figure 4. Block diagram of atomic absorption system

Table 4. Description of components of emission and absorption systems

Component	Description
Monochromators	1.0 m Czerny-Turner mount Jarrell-Ash Model 78-462 scanning spectrometer. Effective aperture, f/8.7. Gratings, 1180 grooves/mm blazed for 2500 Å and 5000 Å. Reciprocal linear dispersion, 8.2 Å/mm in first order
	0.5 m Ebert mount Jarrell-Ash Model 82-000 scanning spectrometer. Effective aperture f/8.6. Gratings, 1180 grooves/mm blazed for 2500 Å and 5000 Å. Reciprocal linear dispersion, 16 Å/mm in first order
Photomultiplier detectors	EMI 6256B. Spectral response type, S13. Approximate useful sensitivity range, 1650 Å-6500 Å
	EMI 9558B. Spectral response type, S20. Approximate useful sensitivity range, 2900 Å-8500 Å
Detector power supply	Model S-325-RM, New Jersey Electronic Corporation (500-2500 V 0-10 mA)
Amplifiers	Princeton Applied Research Corporation lock-in amplifier model HR-8
	Leeds and Northrup 9836-B micro-microammeter
	Keithley Model 417 high speed picoammeter

Table 4 continued

Component	Description
Mechanical chopper	Princeton Applied Research Corporation Model BZ-1 mechanical light chopper
Recorder	Leeds and Northrup Speedomax G Model S millivolt recorder
Primary Sources	Sylvania type DXL tungsten filament lamp, quartz envelope, iodine vapor filled
	Hollow cathode tubes

The ethanol-water and aqueous solutions of the metal chlorides or perchlorates were prepared from reagent-grade chemicals. Chloride salts (6, 113) as well as perchlorate salts are generally readily volatilized in flames. The phosphate, borate, and sulfate solutions added to the test solutions to provide a range of anion/cation mole ratios were prepared from their corresponding acids. Aluminum chloride and perchlorate were prepared from aluminum powder.

A continuously variable infusion pump (model 600-000, Harvard Apparatus Co.,Inc., Dover, Mass.) operating at a rate of approximately 1 ml/min was used for all experiments with the premixed O_2-N_2-C_2H_2 burner.

The flame conditions employed to study the alkaline earth-aluminum interference systems were chosen to maximize the sensitivity for barium; other elements were studied under the same conditions for comparison purposes. All spectral signals were measured at an observation height of 20 mm above the burner; aqueous solutions of 25 μg metal/ml served as samples. The ion line intensities recorded on Figures 9-14 are very nearly proportional to free-ion number densities. In the slot burner flames, Ba(I) emission and absorption are also proportional to free barium atoms; however, sufficient self-absorption was present in the studies with Mg, Ca, and Sr so that free-atom emission and absorption signals are proportional to the square root of the free-atom number densities (63).

Results and Discussion

The alkaline earth-anion interference systems

The calcium-phosphate interference system was reinvestigated in the Beckman burner turbulent flame. In the discussion above, attention was called to several severe limitations imposed by Beckman turbulent flames toward the minimization of chemical interferences. In spite of these limitations, the reinvestigation of the depression of the calcium emission by increasing phosphate concentrations revealed an unexpectedly small depressant effect when water solvent was used, and no detectable depression for an ethanol-water mixed solvent. In Figure 5, the reinvestigation results are graphically compared with typical literature data. It is apparent from Figure 5 that up to molar ratios (PO_4/Ca) of 100, no interference was observed when ethanol-water solutions were employed, and only a 14% depression was detected for water solvents. These observations are in contrast to the depressions of the calcium emission signal from 36 to 54% reported by previous investigators.

The absence of significant interference when ethanol-water solutions are nebulized may simply reflect the beneficial actions of organic solvents in reducing chemical interference effects. Since the oxy-hydrogen flame employed in two of the studies mentioned in Figure 5 (132, 137) is approximately

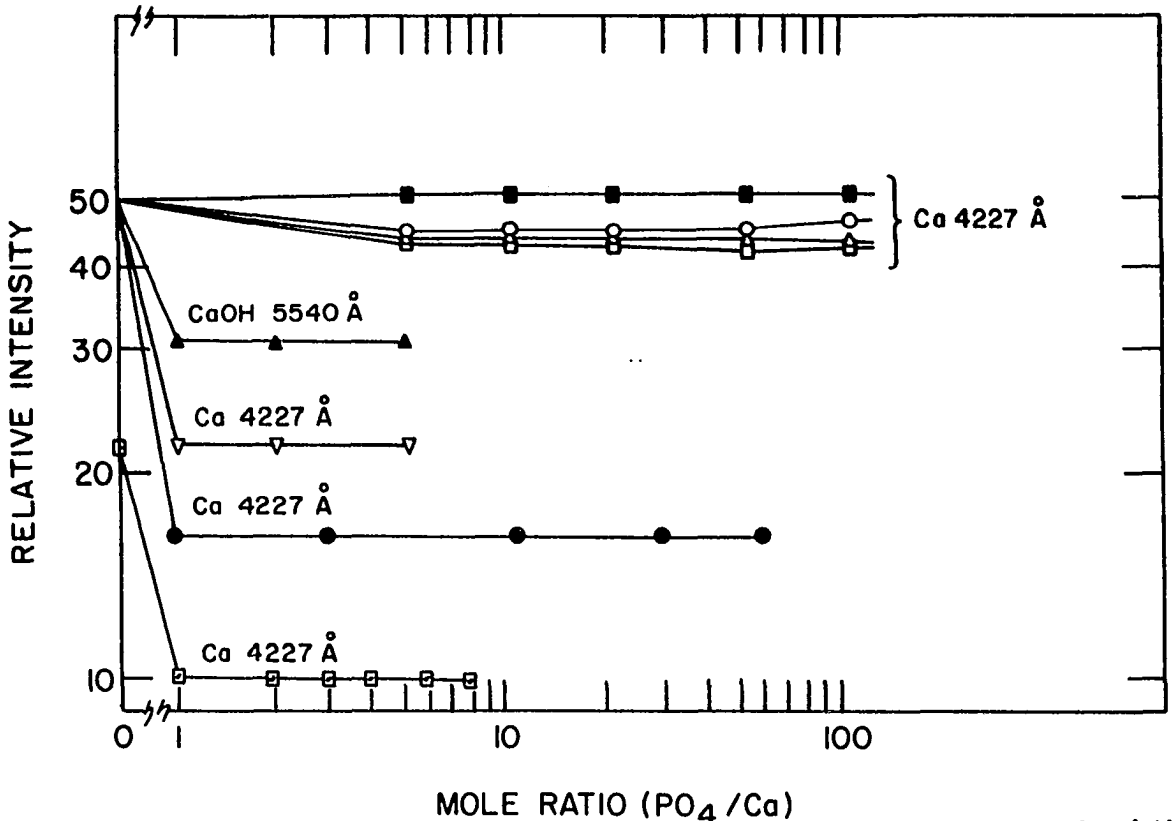

Figure 5. Comparison of phosphate interference effect as observed with a Beckman burner. Reinvestigation results using 25 μgCa/ml: 1:1 ethanol-water solvent, 20 mm above primary reaction zone (■); water solvent at 15 mm (○), 5 mm (△), and zero mm (□) above the primary reaction zone. ▲ from reference 12, ▽ from reference 132, ● from reference 34, and ⊡ from reference 137

300 ^{o}K cooler than its oxy-acetylene counterpart (61, p. 77), the higher degree of interference in the former flame may also be reconciled. However, a comparison of pertinent experimental conditions indicated in the publications does not give any sound basis for expecting the much lower degree of interference under the environmental conditions employed herein. There is, for example, no apparent logical basis for the disagreement in the magnitude of the depression for the Dippel (34) and Baker and Johnson (12) results for oxy-acetylene flames. Thus, the alignment of the experimental results in Figure 5 strongly suggests that: (a) an observed chemical interference effect may be so unique that there is little expectation of precise duplication of the degree of depression by other investigators, and (b) that subtle differences in the experimental conditions may play a very significant role in establishing the degree to which a chemical interference may occur.

The focus of the present discussion is not primarily concerned with the question of whether quantitative agreement on interference effects can be achieved by different investigators. Of far greater importance is the question of whether an interference can be easily and confidently eliminated. As noted above, the recent development of burners capable of providing high temperature premixed flames has given the analyst a greater opportunity of directly eliminating many

interferences of this type. Since these same flames are destined to replace the turbulent versions as excitation sources, there is a compelling reason for evaluating their capability in completely eliminating one of the much publicized interferences.

Figure 6 shows that even at the 200 μg Ca/ml level, no significant depression of the calcium emission signal occurs up to PO_4/Ca molar ratios of 100 for O_2-N_2-C_2H_2, N_2O-C_2H_2, and O_2-C_2H_2 flames under the experimental conditions specified in the figure caption. At molar ratios greater than 100, the solids content of the solution significantly affected the physical properties of the solution so that the nebulization efficiency was altered. Thus, the depression in emission beyond molar ratios of 100 should not be completely assigned to a vaporization or chemical interference effect. For comparison purposes, the interference effects observed in several previous investigations are also shown on the figure. Results similar to those shown in the top two curves of Figure 6 were obtained for aqueous solutions nebulized into the N_2O-C_2H_2 flame. The calcium-phosphate interference doesn't appear to depend on flame stoichiometry or observation height in the N_2O-C_2H_2 flame. The interference curves obtained by atomic absorption are similar to those obtained by emission, thus refuting the claim that flame atomic emission is more susceptible to these interferences than atomic absorption

Figure 6. Comparison of phosphate interference on calcium. Present investigation: premixed O_2-C_2H_2 slot burner (○), premixed N_2O-C_2H_2 slot burner (□), premixed O_2-N_2-C_2H_2 burner (◇), all measurements made at 20 mm above the burner with 200 μg Ca/ml in 1:1 ethanol-water nebulizing. From reference (8): air-C_2H_2 indirect nebulizer burner with 116 μg Ca/ml in water nebulizing at 112 mm (△) and 32 mm (▽) above the inner cones

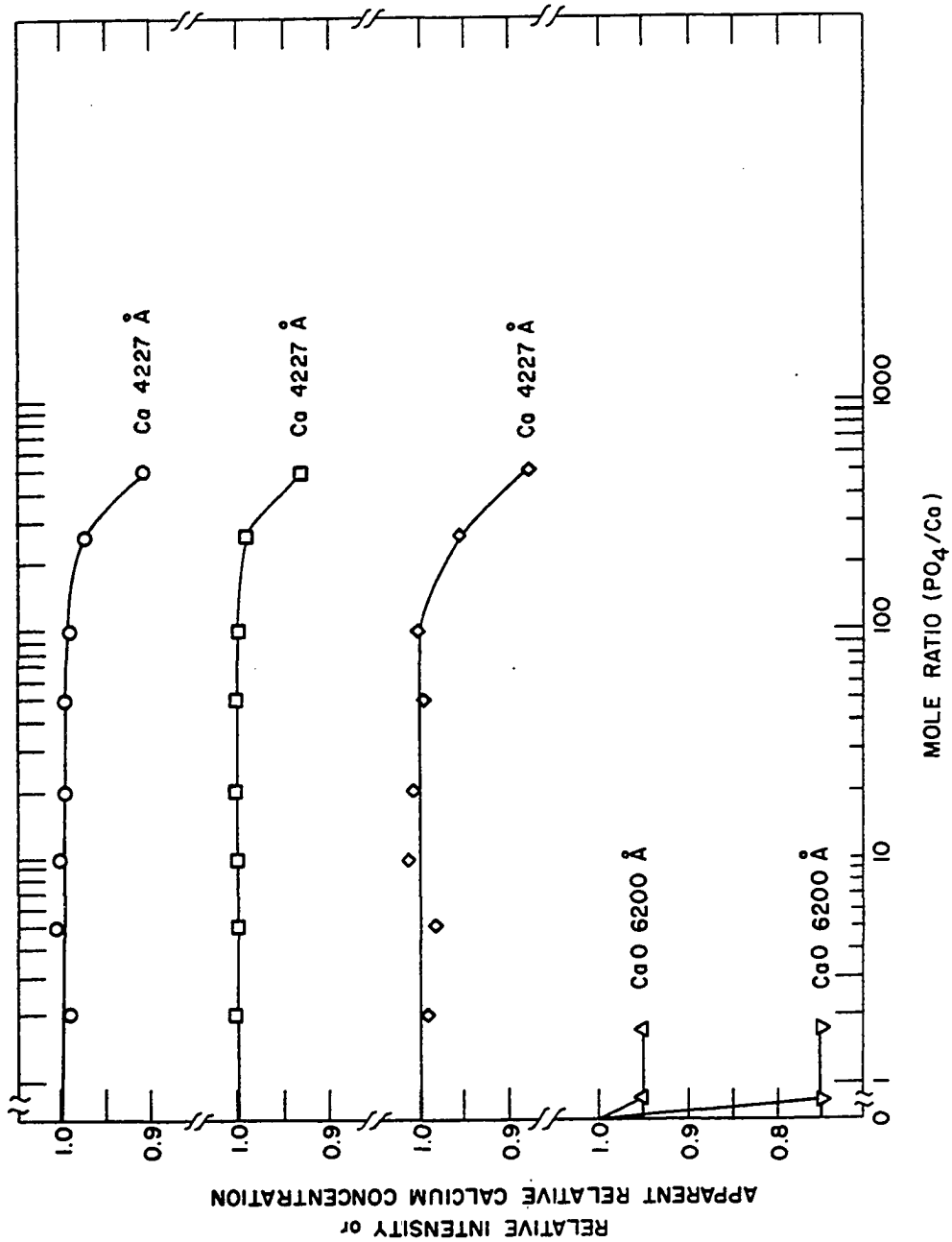
Ca 4227 Å
Ca 4227 Å
Ca 4227 Å
CaO 6200 Å
CaO 6200 Å
1.0
0.9
1.0
0.9
1.0
0.9
1.0
0.8
0
1
10
100
1000
MOLE RATIO (PO_4/Ca)
RELATIVE INTENSITY or
APPARENT RELATIVE CALCIUM CONCENTRATION

(134).

Figure 7 shows that no significant interference effect of phosphate ion on magnesium, strontium, and barium emission was observed below molar ratios of 500 in the premixed O_2-N_2-C_2H_2 flame when 1:1 EtOH-H_2O solvent was employed. Analogous results were obtained in the N_2O-C_2H_2 slot burner flame in emission. For comparison purposes, the typical depression effect observed in Beckman turbulent flames are shown in the figures. In a paper published after the initial disclosure (42, 43) of the results summarized above, Mossotti and Duggan (98) presented data obtained with a N_2O-C_2H_2 premixed total consumption burner, which are in complete accord with the observations reported herein. Thus the Mossotti and Duggan results and the experimental data summarized in Figures 5 to 7 clearly show that one of the most notorious chemical interferences effects, whose description has occupied so much space in the literature, may be either completely eliminated or reduced to negligible proportions through the proper selection of environmental conditions. It is of interest to note that certain reports in the atomic absorption literature (9, 87, 120) confirm some of the emission observations summarized above, whereas other absorption reports (10, 90) indicate that phosphate enhances calcium absorption rather than exerting the classical depressant effect.

The depression of calcium emission by increasing

Figure 7. Comparison of phosphate interference on Mg, Ba and Sr

○ This investigation: observations in interconal zone of premixed O_2-N_2-C_2H_2 flame; 25 μg of metal/ml in 1:1 ethanol-water

□ From reference 34 and

◇ From reference 137

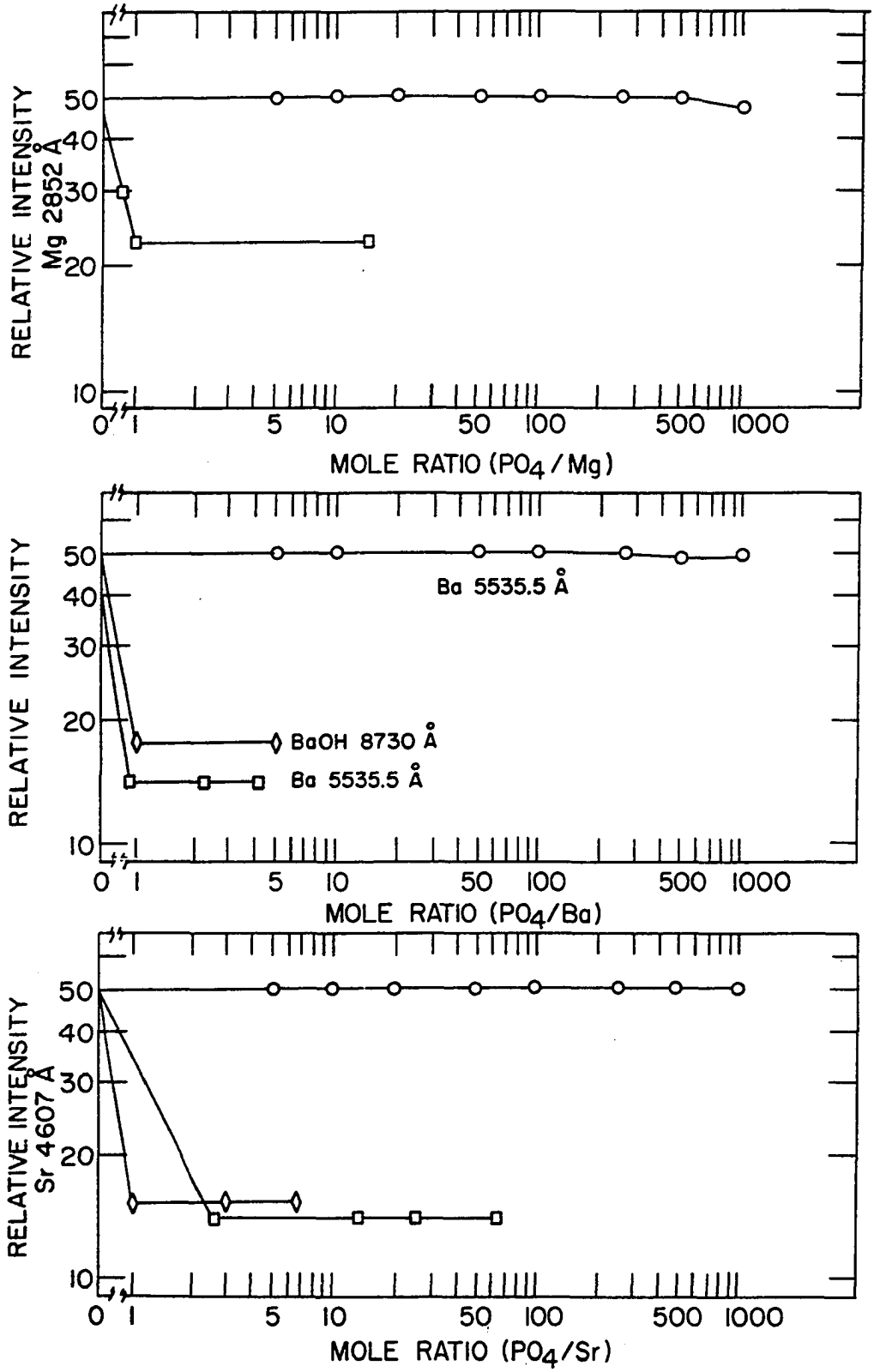
RELATIVE INTENSITY
Mg 2852 Å
50
40
30
20
10
0
1
5
10
50
100
500
1000
MOLE RATIO (PO4 / Mg)
RELATIVE INTENSITY
Ba 5535.5 Å
BaOH 8730 Å
Ba 5535.5 Å
MOLE RATIO (PO4/Ba)
RELATIVE INTENSITY
Sr 4607 Å
MOLE RATIO (PO4/Sr)

concentrations of sulfate and borate ion has also been recorded in the literature. In Figure 8, the degree of depression of calcium emission by sulfate as observed in the premixed O_2-N_2-C_2H_2 flame is compared with observations made by various investigators in Beckman burner turbulent flames. Again the present investigation shows that no interference is evident below a sulfate/calcium molar ratio of 500. Analogous results were obtained with the N_2O-C_2H_2 slot burner flame with 1:1 ethanol-water solutions nebulizing. The borate interference, which has been reported to be similar to the sulfate interference in its depressant effect (36), is also virtually non-existent in the premixed O_2-N_2-C_2H_2 flame and N_2O-C_2H_2 slot burner flame.

The alkaline earth-aluminum interference systems

The alkaline earth-aluminum interference systems present a more formidable challenge for those interested in coping with condensed-phase chemical interferences. The magnitude and persistence of this interference in relatively low temperature flames or flames provided by direct nebulizer-burners are aptly illustrated in the literature (8, 36, 91). The persistence of the alkaline earth-aluminum interferences is manifested by the rather insensitive dependence of the magnitude of the interference on the height of observation at which the interference studies are made (8, 48); the magnitude of most common alkaline earth-anion interference effects is

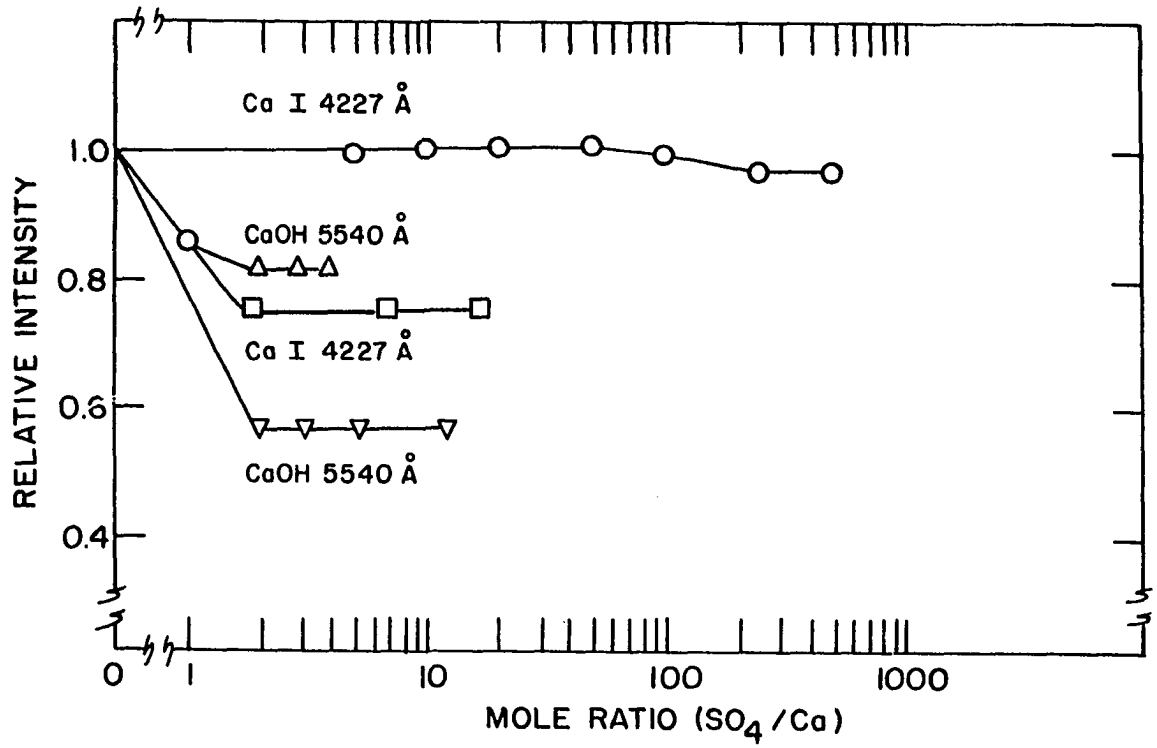

Figure 8. Comparison of sulfate interference on calcium

○ This investigation: observations in interconal zone of premixed O_2-N_2-C_2H_2 flame, 25 μg Ca/ml in 1:1 ethanol-water nebulizing

△ From reference 12; □ from reference 132, and ▽ from reference 137

strongly dependent on the observation height (8, 48). The use of high temperature flames in combination with indirect nebulizer-burners has led to the mitigation of the magnesium-aluminum solute vaporization interference (10, 56, 100). However, magnesium doesn't behave as the other alkaline earth metals in the presence of aluminum. A fairly severe calcium-aluminum interference has been reported in the N_2O-C_2H_2 slot burner flame (110).

An investigation of the calcium-aluminum interference system in the nitrous oxide-acetylene slot burner flame resulted in the interference curves presented in Figure 9. The data in Figure 9 indicate a slight enhancement in the calcium free atom density at low aluminum concentrations. Such enhancements are not a characteristic of condensed-phase interferences; however, the precipitous decrease in the calcium ion population suggests that a second process is occurring which affects the interference curves. Evidently an ionization effect as well as a solute-vaporization effect is responsible for describing the interference system. Since the ionization energy of aluminum is only 5.96 eV (53), aluminum is capable of increasing the electron density in the flame. The relative increase in the electron number density shifts the ionization-recombination balance of the calcium toward the formation of increased amounts of free calcium atoms. A solute-vaporization inhibition would tend

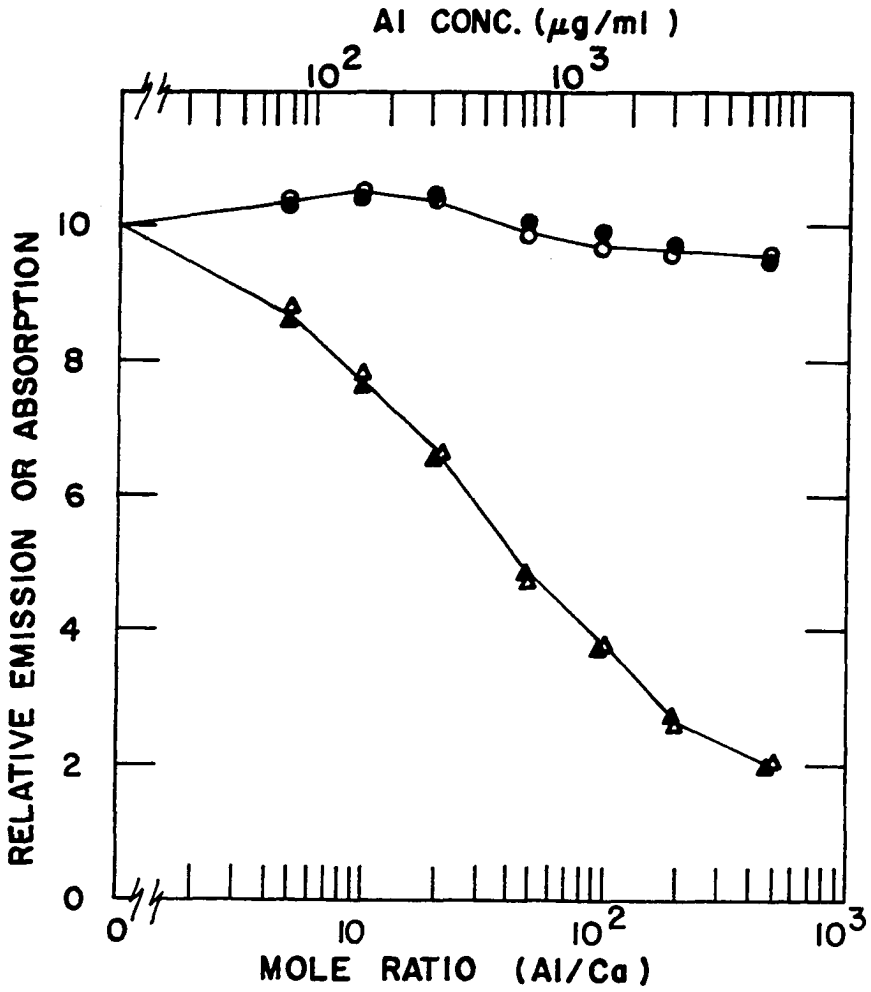

Figure 9. Al on Ca interference in the N_2O-C_2H_2 slot burner flame. Ca(I) (λ= 4227 Å) emission (○) and absorption (●). Ca(II) (λ= 3934 Å) emission (△) and absorption (▲)

to decrease the calcium atom and ion number densities as a function of interferent concentration, whereas an ionization effect would tend to increase the calcium atom number density and decrease the calcium ion number density.

The ionization effects can be separated from the solute-vaporization effects in order to determine the relative importance of these two processes in the description of the interference curves. If the analyte and interferent are introduced into the flame using the separate nebulization technique (7, 48), the solute-vaporization effect is virtually non-existent and only ionization effects should describe the interference curves. If the intrinsic ionization of the analyte is buffered by the addition of an excess amount of some easily ionizable element (e.g., potassium), then under this condition of complete analyte ionization suppression the addition of some interferent (e.g., aluminum) will not affect the ionization of the analyte; only the solute-vaporization effect will appear in the interference curve. These two techniques, separate nebulization and ionization suppression, allow the determination of the relative contribution of solute vaporization and ionization to the description of the interference curves.

Figure 10 shows the importance of ionization and solute vaporization in the description of the calcium-aluminum interference system. Under the condition of separate

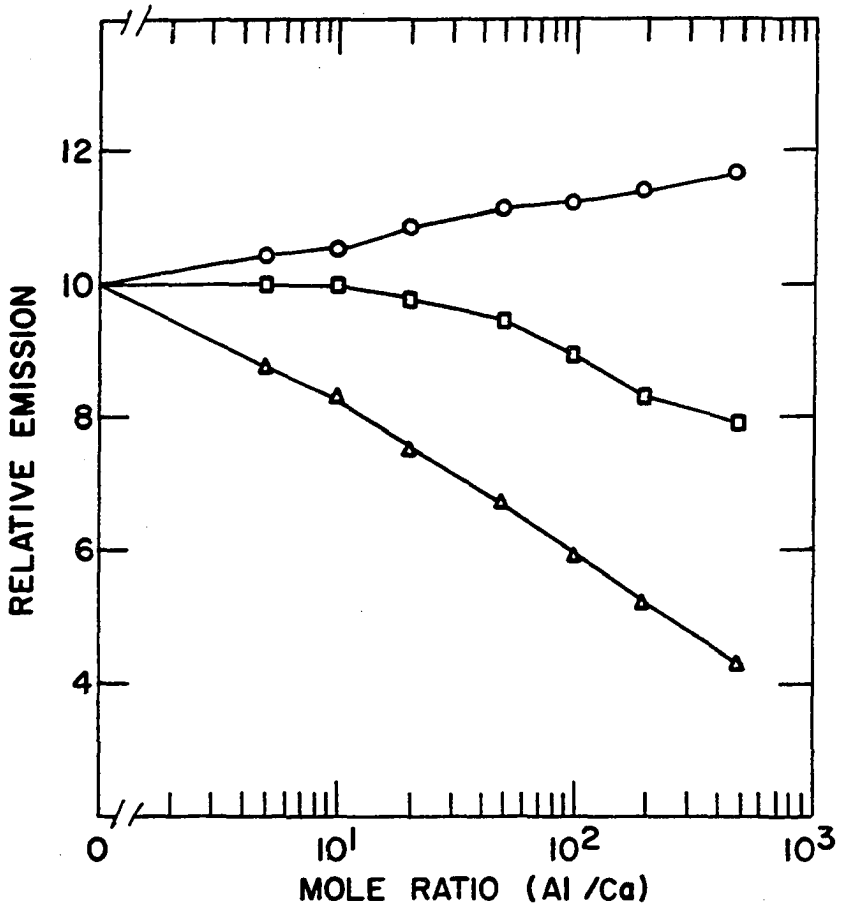

Figure 10. Al on Ca interference in the N_2O-C_2H_2 slot burner flame. Separate nebulization: Ca(I) (λ = 4227 Å) (O) and Ca(II) (λ = 3934 Å) (Δ). Ionization suppression: Ca(I) (λ = 4227 Å) (□)

nebulization, the calcium atom concentration increases monotonically as expected. Aluminum starts to inhibit the vaporization of the aerosol droplet at a mole ratio of 20 (approx. 300 μg Al/ml). If the ionization curves in Figure 10 are corrected for the vaporization effect determined by the ionization suppression method, the curves presented in Figure 9 result. For the determination of the ionization suppression curve in Figure 10, the addition of the buffer may be accomplished by either direct addition to the sample solution or by the separate nebulization technique.

Ionization effects can be handled very simply by the analytical spectroscopist. The addition of an ionization buffer (e.g., KCl) in excess amounts can completely predominate the ionization picture while offering no additional apparent solute-vaporization problems. To further reduce solute-vaporization effects, a higher degree of optimization of certain flame parameters must be considered. Figure 11 presents the calcium-aluminum vaporization interference in the oxy-acetylene flame. The vaporization effect is negligible up to aluminum concentrations in excess of 1000 μg Al/ml.

The behavior of other alkaline earth-aluminum interference systems is not similar to the calcium system. The relative enhancements in free-atom emission or absorption depends on the initial fractional ionization of the analyte. Table 5

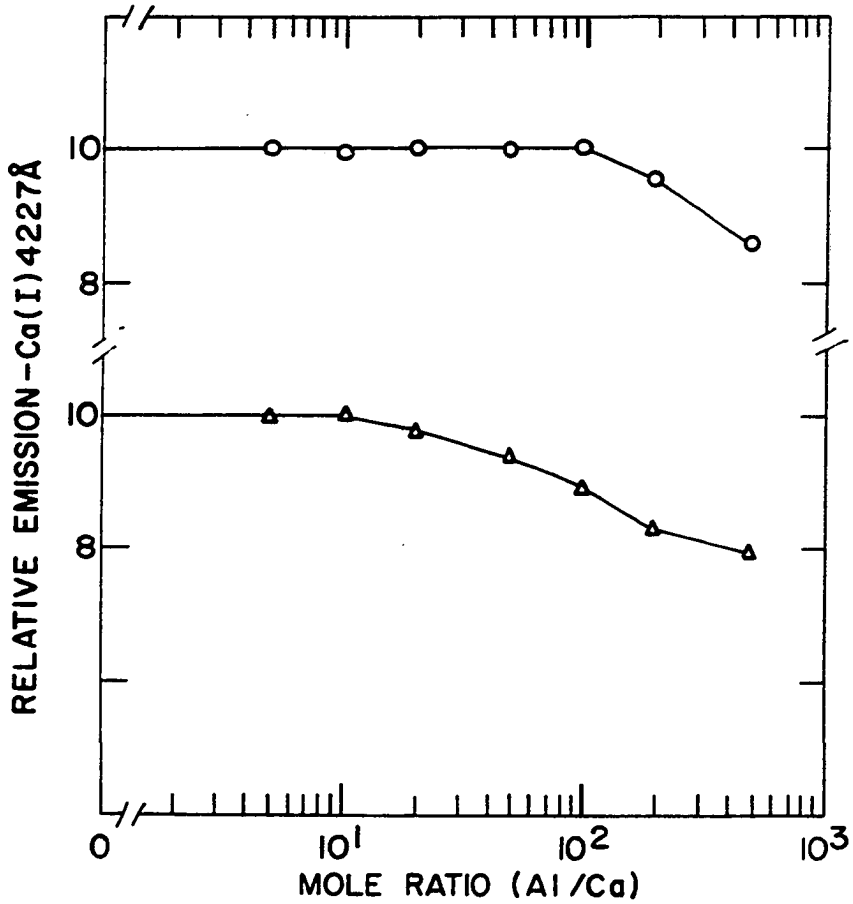

Figure 11. Al on Ca interference in two slot burner flames. Ionization suppression: O_2-C_2H_2 flame (O) and N_2O-C_2H_2 flame (Δ)

lists the fractional ionizations of the four analyte metals studied here.

Table 5. Fractional ionizations[a] for 25 μg metal/ml at an observation height of 20 mm in the N_2O-C_2H_2 slot burner flame

Mg	Ca	Sr	Ba
<.02	.30	.68	.85

[a]The determination of fractional ionizations is discussed in Chapter III.

The solute-vaporization effect of aluminum on barium and strontium is similar to the calcium-aluminum system. However, ionization should play an increasingly important role for the strontium and barium interference systems since the free atom populations should undergo greater relative changes as the analyte ionization is being suppressed by the interferent. The strontium-aluminum and barium-aluminum interference curves are presented in Figures 12 and 13.

The magnesium-aluminum interference system is remarkably different from the other alkaline earth-aluminum interferences. Magnesium is ionized less than 2% in the nitrous oxide-acetylene flame and in the oxy-acetylene flame (see Table 5). Thus the magnesium-aluminum interference curves which are presented in Figure 14 should not indicate an enhancement in the Mg(I) signal at increasing interferent concentrations.

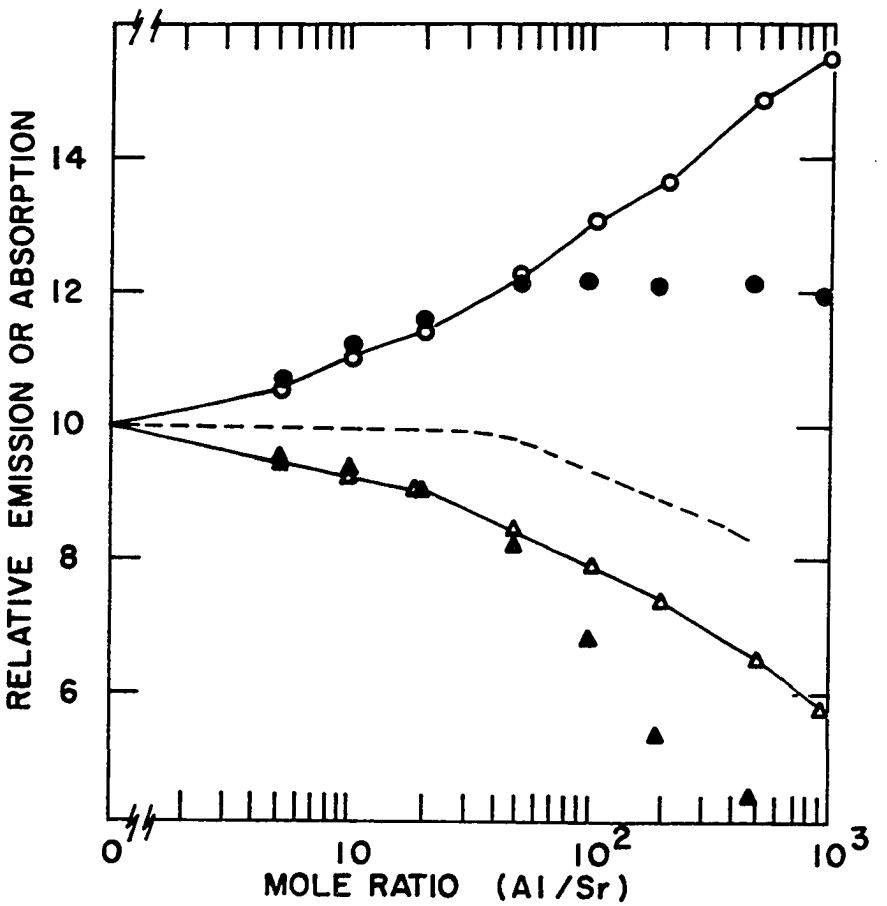

Figure 12. Al on Sr interference in the N_2O-C_2H_2 slot burner flame. Sr(I) (λ = 4607 Å) emission or absorption (●). Sr(II) (λ = 4078 Å) emission or absorption (▲). Separate nebulization: Sr(I) (○) and Sr(II) (△) emission. Ionization suppression: Sr(I) emission (---)

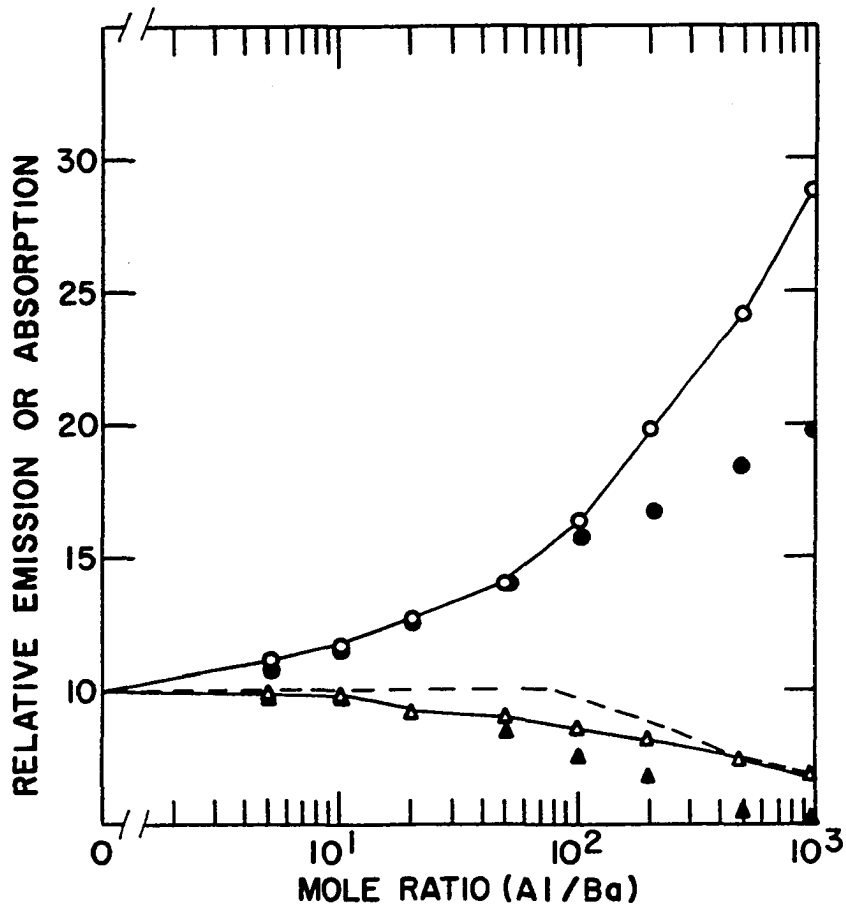

Figure 13. Al on Ba interference in the N_2O-C_2H_2 slot burner flame. Ba(I) (λ = 5535 Å) emission or absorption (●). Ba(II) (λ = 4554 Å) emission or absorption (▲). Separate nebulization: Ba(I) (○) and Ba(II) (△) emission. Ionization suppression: Ba(I) emission (---)

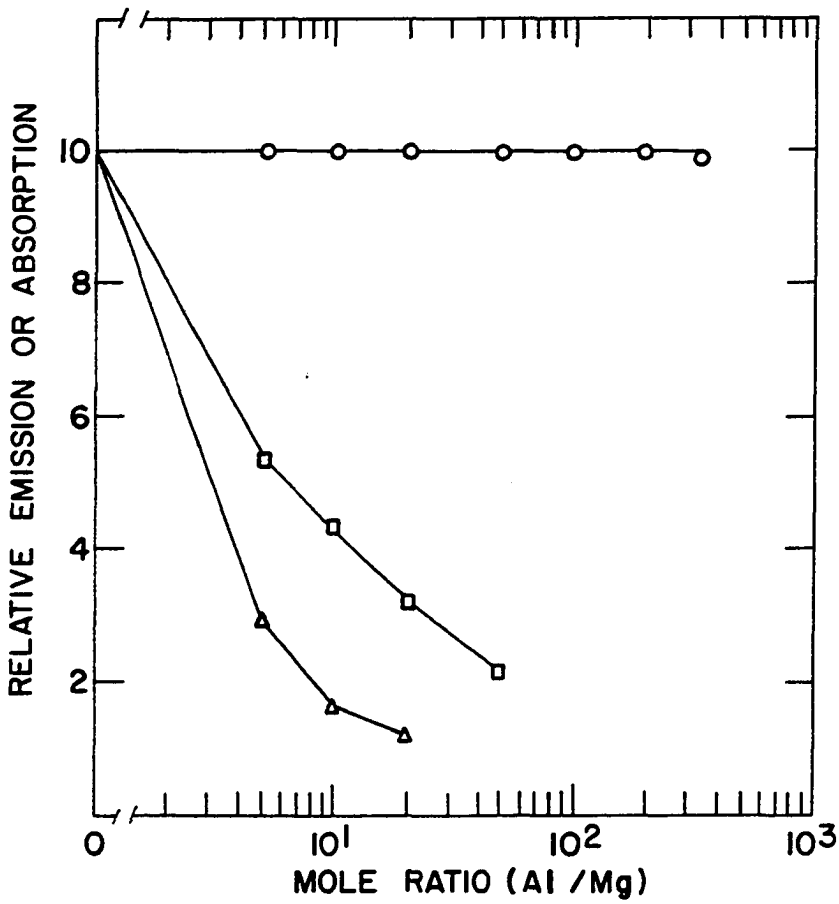

Figure 14. Al on Mg interference in two slot burner flames. Mg(I) (λ = 2852 Å) emission or absorption (O): O_2-C_2H_2 flame and N_2O-C_2H_2 flame. Mg(II) (λ = 2796 Å) emission: O_2-C_2H_2 flame (□) and N_2O-C_2H_2 flame (Δ)

The precipitous decrease in Mg(II) emission results because the magnesium ion number density represents a small fraction of the total magnesium present. The magnesium free-ion number density is more sensitive to added aluminum in the nitrous oxide-acetylene flame than in the oxy-acetylene flame. Evidently the relative increase in the electron number density upon the addition of aluminum is greater in the N_2O-C_2H_2 flame. If the electron concentration in the unsalted O_2-C_2H_2 flame significantly exceeds that in the N_2O-C_2H_2 flame, an ionization interferent would sensibly affect an analyte's ionization to a greater extent in the N_2O-C_2H_2 flame. The complete elimination of the magnesium-aluminum vaporization interference in the nitrous oxide-acetylene flame has been reported by other investigators (10, 100) and is in marked contrast with the behavior of other alkaline earth-aluminum vaporization interferences under similar experimental conditions. The variation in the aluminum vaporization interferences from magnesium to the other alkaline earths is difficult to rationalize since aluminum emission, at high concentrations where a calcium-aluminum vaporization interference exists, is not affected by small amounts of calcium or magnesium.

The interference investigation described herein proves that several of the so-called condensed-phase or solute-vaporization chemical interferences can be eliminated by optimization of several experimental variables. However,

the ionization of metals, which are introduced into flames, becomes increasingly important as steps are taken to reduce or eliminate condensed-phase chemical interferences. Thus, the chronology of events leads to the experimental investigation of metal additive ionization presented in Chapter III.

CHAPTER III. IONIZATION

Introduction

The observation of charged species in hydrocarbon flames dates back to the early part of the last century (19, 94). The early experimenters noted that hydrocarbon flames were deflected by strong electric fields and that these flames were capable of conducting an electric current. The identification of ions and electrons in flames led to the supposition that these species were important in the flame propagation processes (50, p. 314; 94). Flame ions are now known to exist in many unsalted or "clean" flames as well as in salted flames.

The experimental investigation described in this chapter considers the observed ionization of metals in the nitrous oxide-acetylene flame in relation to equilibrium ionization. Since metal ionization is influenced by the ionization of natural flame species, the electron number density in a clean flame must also be considered in an analysis of metal ionization. Considerable background material regarding ionization in flames as well as equilibrium considerations will be presented in order that the subject of flame ionization and related effects may be more fully discussed.

If thermodynamic equilibrium prevails in flames, the mechanism of ion formation is designated as thermal and

the ionization conforms to the Saha equation (115). The concentrations of the stable ions can then be calculated by applying the Saha equation to the equilibrium amounts of the combustion products, which are calculable from thermochemical data. However, general thermodynamic equilibrium does not prevail in chemical flames (5; 50, p. 228; 66; 67).

The following criteria must be met in order for thermodynamic equilibrium to be established (38):

1. The velocity distribution function of all particles is Maxwellian.
2. The population density of the excited states is Boltzmannian.
3. The distribution of the molecules and their dissociation products obeys the mass action law of Guldberg and Waage.
4. The distribution of the atoms and their ionization products obeys the Saha-Eggert equation.
5. The electromagnetic radiation field has a Planckian distribution, where the radiation temperature equals the kinetic temperature of the reacting particles.

The preceding criteria may be summarized by stating that a volume of gas is in thermodynamic equilibrium at a given temperature when this temperature describes: (a) the distribution of energy in the internal and external forms or "degrees of freedom" of the gas, (b) the degrees of ionization and dissociation of the gaseous species, and (c) the radiation density in the volume of gas (66).

Of the five criteria, which define thermodynamic equilibrium in a plasma, the requirement of Planckian radiation is most obviously not met by the flame gases. A Planckian radiation distribution is only possible for a blackbody radiation source. If a flame were a blackbody source, flame spectroscopy would not be feasible. Over most of the wavelength region of interest to flame spectroscopists, the flame gases are nearly transparent or optically thin. Only in narrow wavelength ranges within which strong emission or absorption occurs can the Planck function be approached. Thus the flame gases must be optically thick in order for the plasma to radiate as a blackbody.

Even though the Planck function fails to describe the radiation from a flame, a single temperature can still describe the chemical balance reactions and the partitioning of energy over the various degrees of freedom. If collision-induced reactions are much more frequent than radiative ones, the actual population of excited states becomes, in effect, the same as that predicted by the Boltzmann equation (5). Therefore, if the rate of energy transfer from the flame is slow relative to the rate at which energy can be partitioned over the various forms, local thermodynamic equilibrium (LTE) can characterize a system at a local temperature.

The state of a chemical flame can now be discussed in terms of local thermodynamic equilibrium. In a premixed flame, two distinct main regions can be discerned. The primary reaction zone, which is generally very restricted in extent, is the region where the main part of the combustion occurs. The sudden burst of energy released in the primary reaction zone leads to high concentrations of reactive species, which exceed the equilibrium amounts (50, p. 228; 67; 127). Local thermodynamic equilibrium cannot possibly describe the state of the primary reaction zone since the chemical energy released in the oxidation process is not equally partitioned over the various degrees of freedom (50, p. 320). The requirements of LTE are more likely to be approached in the secondary reaction zone where the violence of the chemical reactions is much subdued.

High temperatures favor high effective collision rates. For this reason, the principles of LTE are commonly applied to electrically generated inert gas plasmas, which are characterized by temperatures on the order of 10,000 kelvins (103). However, the temperatures of most chemical flames are approximately 3000 ^{o}K or less. Therefore, the time available for the chemical reactions to occur is of primary importance when considering the approach to LTE in flames.

In order for LTE to be established in the secondary reaction zone, the energy released in the primary oxidation must be equally partitioned over the various forms, and chemical reactions must occur rapidly relative to the rise velocities of the gas molecules through the flame. A typical rise velocity for flame gas molecules is 10 m/sec. Since measurements are performed at observation heights of approximately 10 mm above the burner tip, flame molecules spend about 1 msec in their chemical environment before their properties are measured. In flames at atmospheric pressure, a flame molecule makes about a million collisions with surrounding molecules in a time interval of 1 msec. The exchange of translational and rotational energy is very effective; equilibrium distributions for these two types of energy should be attained after about one to ten collisions (5). The distribution of energy over vibrational forms is a slower process than the exchange of translational or rotational energy. However, serious deviations from an equilibrium distribution of vibrational energy are not expected (5; 49, p. 201). The mechanism of formation of electronically excited atoms and molecules in combustion flames is somewhat unsettled. Transfer of translational energy from flame molecules or electrons to the species of interest is unlikely to account for appreciable excitation (5; 50, p. 218; 71). Transfer of internal vibrational

energy from molecular species is probably the most important mechanism of electronic excitation. Small amounts of translational and rotational energy may accompany the vibrational energy in order to make the available-energy distribution more continuous. If the energy is equi-partitioned over the vibrational forms of energy, the energy may also be considered to be distributed over electronic degrees of freedom in an equilibrium manner (124).

The preceding brief survey concerning energy exchanges suggests that the non-equilibrium energy distributions in the primary reaction zone are rapidly equilibrated in the secondary reaction zone. The Boltzmannian and Maxwellian distribution functions will describe the distribution of internal and translational energy if lags in the chemical balance reactions do not appreciably affect the energy distributions. The slight radiation disequilibrium inherent in flame was previously discussed in terms of deviations of a flame from a blackbody radiator. In most hydrocarbon flames, radiative disequilibrium affects the Boltzmann population distribution by only a few per cent (71). If the Boltzmann and Maxwell relationships hold in the secondary reaction zone of a flame, "thermal equilibrium" exists in this region.

The non-equilibrium amounts of reactive species formed in the primary reaction zone of many flames must approach their respective equilibrium amounts in the secondary

reaction zone if the remaining criteria for establishing LTE are to be fulfilled. Over-equilibrium amounts of radicals, which exist in the primary reaction zone (5; 50, p. 228; 67; 127; 138), generally react in one of two ways: (a) rapid bimolecular exchange reactions result in steady-state balances of the radicals while causing no net change in the total radical concentrations (77) and (b) relatively slow termolecular recombination reactions (49, p. 202) decrease the radical concentrations until equilibrium amounts of the radicals exist. However, the equilibrium amounts of the radicals change continuously with time and full equilibrium with respect to the chemical reactions of natural flame species may never be attained.

The deviations that exist between the observed amounts of reactive radicals and the equilibrium amounts in the primary reaction zone suggest that the ionization products may not be equilibrated in this region of many flame systems. If the ionization relaxation processes are sufficiently slow, the effects of non-equilibrium ionization will be observed in the secondary reaction zone too. The ionization of natural flame species will be discussed in light of information published in the literature. Metal ionization in salted flames will be discussed in a review of the literature as well as in an experimental study of metal ionization in the nitrous oxide-acetylene flame.

Literature Review of Natural Flame Species Ionization

Introduction

Increased emphasis has been placed on flame ionization research during the past two decades. Undoubtedly, the investigation of combustion products in rocket exhaust gases benefited flame ionization research. Free electrons in the exhaust gases are responsible for the attenuation and reflection of communication signals. Chemical kineticists have derived information regarding ion-molecule reactions in flames. Flames are particularly convenient for studying chemical kinetics because the temperature, composition, and pressure of flame systems are easily controllable.

Ions in flames may originate through two mechanisms; the most familiar mechanism is equilibrium or "thermal" ionization. The micromechanisms of thermal ionization need not be known to evaluate the thermal ionization constant or Saha constant; knowledge of the temperature and only a few basic properties of the ionizing species are required.

The early theories of ion formation in flames favored the thermal or equilibrium mechanism. Calcote (22) and van Tiggelen (130) indicated that the ion precursor for thermal ionization must possess an ionization energy between about 2 to 4 eV in order to account for the temperature dependence of ion number densities. The thermal theory was always somewhat nebulous since no direct evidence for species

possessing sufficiently low ionization energies was presented. Possible ionizable flame species include: (a) impurities, (b) equilibrium or non-equilibrium amounts of flame molecules and radicals, (c) long chain carbon-hydrogen compounds, and (d) carbon particles. Ionization of impurities can be ruled out since they don't exist in sufficient quantity (19). Flame molecules and long chain hydrocarbons are improbable precursors to thermal ions because of the extremely high ionization energies of these species. The ordinary equilibrium flame gas molecules such as O_2, N_2, H_2O, CO, CO_2, OH, H, O, etc., are characterized by ionization energies ranging from 12 to 16 eV (50, p. 303). Unstable radicals such as CH and C_2 possess ionization energies that range from 11-13 eV (19). The ionization energies of hydrocarbons decrease with increasing molecular weight and increasing unsaturation (50, p. 322). However, equilibrium amounts of high carbon-number hydrocarbons are generally insignificant in non-luminous flames and low carbon-number hydrocarbons possess ionization energies that approach the ionization energies of flame radicals.

Another possible source of thermal ions is carbon particles. In luminous premixed flames, carbon conglomerates or soot particles are probably created by surface decomposition of hydrocarbons on active carbon nucleii (49, p. 189), which appear to be formed from carbon radicals and acetylene.

The intermediate reactions leading to carbon formation involve polyacetylene compounds as well as polycyclic aromatic compounds (70). The soot formation process, which is non-equilibrium in nature, leads to partly-cyclic compounds, which contain carbon and trace amounts of hydrogen and oxygen (44). If the carbon particles become sufficiently large, the soot should have a characteristic ionization energy approaching that of graphite (4.35 eV) (85). The electron density is indeed appreciably greater in luminous or soot-forming flames than in non-luminous flames (128); however, most ion-producing flames are not operated under the conditions required for soot formation. Graphitic carbon is virtually non-existent in stoichiometric hydrocarbon flames where ion number densities approach values of 10^{12} cm^{-3} (85). Thus, the lack of appropriate thermal ion precursors in flames has placed the thermal ionization mechanism in jeopardy.

A second mechanism, which must be responsible for the ionization of natural flame species, is referred to as chemi-ionization. Chemi-ionization may be defined as a mechanism by which energy available from a chemical reaction produces ionization and rearrangement of the reactants (94). Although an abundance of information in the early literature suggested that chemi-ionization was indeed the mechanism of ion formation in unsalted flames, H. F. Calcote (19) was

the first to insist on such a mechanism. Three general processes, which describe the reactions of chemi-ions, include: (a) primary ion formation, (b) ion-molecule reactions, and (c) recombination. Primary ion formation and ion-molecule reactions occur exclusively in the primary reaction zone of ion-producing flames. Recombination is a slower process and occurs throughout a major portion of the secondary reaction zone.

In order to investigate the chemi-ionization processes, the Langmuir probe technique (24) and mass spectrometric analyses (21, 29, 30, 82, 84, 85) were employed in following ionization reactions in flames. The mass spectrometer was originally considered a panacea for all unresolved problems associated with ionization in flames. Although detailed ion profiles indicated dominant ions and precursor ions, the whole issue was further complicated by the very large number of ionic species observed.

Primary ion formation

A mass spectrum of ions existing in the primary reaction zone of hydrocarbon flames indicates that the ion formation processes are indeed very complex. Mass peaks occur at nearly every mass number from about mass 15 to mass 150. In searching for a plausible primary ion formation reaction then, attempts were made to identify only the dominant ion formation process.

The reactants in a chemi-ionization reaction should meet several criteria that include: (a) large heats of formation, (b) simple species known to exist, (c) species derived from fuel and oxidant, and (d) species that give rise to simple ions, which have been confirmed mass spectrometrically (22). If the reactants possess large heats of formation, the chemi-ionization reaction will approach thermo-neutrality; this factor leads to an increased effective collision rate.

The listing of possible chemi-ionization reactions in unsalted flames can be shortened by noting that there is no significant ionization in O_2-H_2 and O_2-CO flames. A previous report of appreciable ion formation in O_2-N_2-H_2 flames (84) was later explained on the basis of the ionization of hydrocarbon impurities (57). Ions are formed in O_2-CH_4 and O_2-CH_3OH flames, whereas insignificant ionization occurs in O_2-HCHO and O_2-HCOOH flames (130). Presumably the exothermicity of the formation of the CO double bond liberates an appreciable part of the required ionization energy. From the remaining suggested chemi-ionization reactions, one must be selected that agrees with experimental observations and the criteria for reactants previously listed.

Most of the experimental observations that led to the currently accepted mechanism of primary ion formation came from studies of the ionization of trace amounts of hydrocarbons added to O_2-N_2-H_2 flames (18). The concentration of

ions formed by adding equimolar amounts of paraffin hydrocarbons to O_2-N_2-H_2 flames is linear with respect to the number of carbon atoms per molecule. Since methane follows this proportionality too, the chemi-ionization process probably involves a reactant containing a single carbon atom. Fuels such as CO and CS_2 generate an undetectable number (less than 10^6 cm^{-3}) of ions in O_2-N_2-H_2 flames. This negative evidence suggests that hydrogen must be present in the reactant containing a single carbon atom. Since acetylenic and olefinic hydrocarbons as well as paraffins yield flame ions, only one hydrogen atom must be required in the carbon-hydrogen reactant. If alcohols serve as additives for O_2-N_2-H_2 flames, fewer chemi-ions result than can be obtained with a paraffin of the same carbon number. For example, equimolar amounts of propanol and ethane generate the same yield of chemi-ions. The implication now is that oxygen is not present in the original carbon-hydrogen precursor to chemi-ionization. Therefore, one reactant almost certainly must be CH; the fuel molecules must be shattered into fragments containing single carbon atoms as the fuel passes through the reaction zone.

The maximum ion concentrations in non-sooting hydrocarbon flames exist at a nearly stoichiometric ratio of the fuel and oxidant. The second reactant in the chemi-ionization reaction must therefore be derived from the oxidant.

Interpretation of several experimental observations suggested that the second reactant must be atomic oxygen (18, 94).

The determination of the reactants, which participate in the predominant primary ion formation process, leads to the following chemi-ionization mechanism proposed by Calcote (20):

$$\text{(III. 1)} \quad CH + O \rightarrow CHO^+ + e^-, \quad \Delta H \sim 1 \text{ eV}$$

The Calcote mechanism has found general acceptance with other flame ionization researchers, and the mechanism is consistent with mass spectrometric data (54). The CH radical in reaction (III. 1) is very likely in the ground electronic state (15, 93).

The early appearance of the $C_3H_3^+$ ion in the flame ion profile suggested that $C_3H_3^+$ may also be a primary flame ion (23, 94). The $C_3H_3^+$ ion is the only chemi-ion whose concentration maximizes in a fuel-rich flame. The following reaction has been suggested for the formation of the alleged primary ion $C_3H_3^+$ (23, 94):

$$\text{(III. 2)} \quad CH^* + C_2H_2 \rightarrow C_3H_3^+ + e^-, \quad \Delta H \sim -1 \text{ eV}$$

However, reaction (III. 2) is not consistent with all experimental observations (93); other mechanisms, which have been proposed to account for $C_3H_3^+$ formation, must be classified under ion-molecule reactions.

The fact that chemi-ionization doesn't occur in the H_2 or CO flames suggests that these flames should be convenient for studying the ionization of metal additives. If the number density of metal ions is equivalent to the number density of electrons in the flame, one variable can be eliminated in the interpretation of the ionization phenomena.

Ion-molecule reactions

The large variety of ions detected mass spectrometrically indicated that ion-molecule reactions occur to produce secondary chemi-ions (23, 94). The predominant chemi-ion generated by natural flame species in all but nearly luminous fuel-rich flames is the H_3O^+ ion. Since the CHO^+ ion is very likely a primary ion, the following ion-molecule reaction must occur rapidly (20):

$$\text{(III. 3)} \quad CHO^+ + H_2O \rightarrow H_3O^+ + CO, \quad \Delta H \sim -2 \text{ eV}$$

Other chemi-ions appearing in appreciable amounts include the hydrates of H_3O^+ as well as $C_3H_3^+$, $C_2H_3O^+$, CH_3O^+, and CH_5O^+. The carbon-containing secondary chemi-ions may be formed by proton transfer or CH^+ transfer from the primary ion, CHO^+. Thus, most secondary ions of major importance may be formed in the following reactions, whose reactants include species known to be combustion intermediates (23, 93, 94):

$$C_2H_2 + RCH^+ \rightarrow C_3H_3^+ + R$$

$$C_2H_2O + CHO^+ \rightarrow C_2H_3O^+ + CO, \quad \Delta H \sim -2.7 \text{ eV}$$

$$CH_2O + CHO^+ \rightarrow CH_3O^+ + CO, \quad \Delta H \sim -0.4 \text{ eV}$$

$$CH_3OH + CHO^+ \rightarrow CH_5O^+ + CO, \quad \Delta H \sim -2.8 \text{ eV}$$

Except for the CHO^+ ion, all carbon-containing chemi-ions are observed only in the primary reaction zone of nearly stoichiometric hydrocarbon flames. These secondary chemi-ions presumably react by oxidative ion-molecule reactions that result in the formation of the predominant ion, H_3O^+ (93).

Negative ions have also been detected mass spectrometrically in flames (45, 83). In hydrocarbon flames negative ions predominate near the base of the primary reaction zone where the total negative ion concentration approaches that of the positive ions (22, 45). However, in the final reaches of the primary reaction zone and in the secondary reaction zone, the total positive ion concentration approaches the electron concentration. Mass spectrometric profiles of negative ion concentrations suggest that electron attachment as well as ion-molecule reactions may be responsible for negative ion formation. In acetylene flames operating at pressures above 10 torr , the C_2H^- ion is the first negative ion to appear in the flame front. In lower pressure acetylene flames ($<$10 torr), the C_2^- ion appears early in

the flame front and decays rapidly in the primary reaction zone. These facts, along with the observation that the total negative ion concentration maximizes in the fuel-rich flame, suggest that C_2^- and C_2H^- are primary negative chemi-ions (23). Possible reactions, which may be responsible for the formation of primary negative chemi-ions, include (23, 94):

$$C_2H_2O^* + e^- \rightarrow C_2^- + H_2O, \quad \Delta H \sim -2 \text{ eV}$$
$$HC_2O^* + e^- \rightarrow C_2^- + OH, \quad \Delta H \sim -0.1 \text{ eV}$$
$$HC_2O^* + e^- \rightarrow C_2H^- + O, \quad \Delta H \sim -1 \text{ eV}$$

Other negative ions that have been observed in the primary reaction zone may be formed via ion-molecule reactions such as the following (94):

$$C_2^- + OH \rightarrow C_2H + O^-, \quad \Delta H \sim 1.1 \text{ eV}$$
$$C_2^- + H_2O \rightarrow C_2H + OH^-, \quad \Delta H \sim 1.3 \text{ eV}$$

Since most negative ions are characterized by low ionization energies (126), the negative ions are quickly transformed into neutral molecules and electrons. It is not likely that negative ions significantly affect metal ionization in the secondary reaction zone of combustion flames.

Recombination

The only positive ion that is present in significant amounts in the secondary reaction zone of nearly stoichiometric hydrocarbon flames is the H_3O^+ ion. H_3O^+ recombines with negative ions or electrons until equilibrium amounts of these species are established. Recombination of H_3O^+ with a negatively charged radical has been suggested (50). However, the electron concentration exceeds the negative ion concentration by about a factor of 1,000 in the secondary reaction zone (81). Thus, H_3O^+ recombination with an electron is more plausible. The following dissociative recombination is generally accepted as the major recombination reaction (20):

$$\text{(III. 4)} \quad H_3O^+ + e^- \rightarrow H_2O + H, \quad \Delta H \sim -6.3 \text{ eV}$$
$$\text{or} \quad H + H + OH, \quad \Delta H \sim -1.2 \text{ eV}$$

The measured rate constant for reaction (III. 4) (20) indicates that non-equilibrium amounts of H_3O^+ persist well into the secondary reaction zone of ion-producing flames. The non-thermal amounts of electrons accompanying H_3O^+ must be considered in an investigation of metal additive ionization.

Ionization of Metals in Salted Flames

Introduction

If metal ionization parallels the behavior of flame radicals and natural flame ions, which are generally present in non-equilibrium amounts throughout the flame gases, deviations from equilibrium metal ionization will be observed. However, if metal ionization parallels the effective dissociation reactions of some gaseous metal monoxide molecules, which are known to be rapid equilibrium reactions (67, 129), Saha ionization of the metal will be established.

The usual approach in the consideration of metal ionization in flames is to assume that the ionization constant ($\underline{K}$) for the ionization-recombination balance

$$M^{o} \rightleftarrows M^{+} + e^{-}$$

is directly calculable from the Saha equation. Then

$$K = K_{S(aha)} = \frac{[M^{+}]\,[e^{-}]}{[M^{o}]}$$

where the brackets refer to absolute concentrations usually expressed as either partial pressures or number densities. The Saha equation relates the thermodynamic equilibrium constant ($\underline{K_S}$) to the total partition functions of the reacting species as follows (97):

$$(III.\ 5)\quad K_S = \frac{Q_i\, Q_e}{Q_a} \exp\,(-E_i/kT)$$

where: K_S = Saha constant = $P(M^+)P(e^-)/P(M^o)$

$P(\ )$ = partial pressure

Q_i, Q_e, Q_a = total partition function for the ion, electron and atom

E_i = ionization energy

k = Boltzmann constant and

T = temperature (kelvins)

Only the translational and electronic partition functions need be considered for metal atom ionization. Thus, (III. 5) reduces to:

$$(III.\ 6)\quad K_S\ (atm\ ) = 6.56 \times 10^{-7} \frac{Q_i^e}{Q_a^e}\ T^{5/2} \exp(-E_i/kT)$$

The major problem in applying the Saha equation is the determination of an accurate temperature of the system. Accurate values for the ionization energies of metals are known. Since the second ionization energies of most elements exceed 10 eV (37, p. 34), only the singly ionized species need be considered in the common chemical flames. The electronic partition functions of the ion and atom,

Q_i^e and Q_a^e, are directly calculable from information presented in atomic energy level tables since the series in the partition function expression neatly converges at temperatures typical of most flames.

Literature review of metal additive ionization

T. M. Sugden and associates studied metal ionization primarily in O_2-N_2-H_2 flames. In these flames, the major alkali-containing ion is M^+ whereas the predominant alkaline earth-containing ion is MOH^+ (82). The early experiments concerned with alkali ionization indicated that a steady-state balance between ionization and recombination was established. The apparent deviation between the experimental ionization constant and the Saha constant was explained by considering the formation of OH^-. Therefore, the ionization of alkalis in the O_2-N_2-H_2 flame was considered to be thermal at this point in the evolution of Sugden's metal ionization research (74, 121-123).

In 1958, Knewstubb and Sugden (86) reported the first observations of infra-thermal amounts of ionization in O_2-N_2-H_2 flames. Cesium and potassium were thermally ionized whereas sodium and lithium ionization lagged the equilibrium amount. Sodium ionization approached thermal predictions more closely than lithium ionization.

The establishment of Saha or equilibrium ionization does not suggest a mechanism for ion formation and recombination. One suggested mechanism of alkali ionization in the O_2-N_2-H_2 flame (107),

$$M + OH \rightleftarrows M^+ + OH^-$$

has been ruled out because OH^- is not stable in the secondary reaction zone of hydrogen flames (105). At one time, the activation energy for the ionization of sodium was reported to be about 2 eV below the ionization energy of sodium in hydrogen flames. The following mechanism for sodium ion formation was proposed to account for the discrepancy between the activation and ionization energies (58, 106, 125, 126):

$$Na + H_2O \rightarrow Na^+ \cdot H_2O + e^- \quad \text{(slow)}$$

$$Na^+ \cdot H_2O + X \rightarrow Na^+ + H_2O + X \quad \text{(fast)}$$

In the preceding ionization scheme, X represents a third body such as N_2. The hydration energy of Na^+ is thought to be on the order of 2 eV; the discrepancy between the activation energy of sodium ionization and the ionization energy of sodium can therefore be reconciled (106). Hydrated alkali ions have been observed mass spectrometrically (82); however, the activation energy discussed above is believed to be in error (76). Moreover, another report indicates that the activation energy of sodium ionization equals the

ionization energy of sodium in the O_2-H_2 flame (130).

The ionization rates of alkali metals in the primary reaction zone of hydrogen flames diluted with one percent acetylene apparently are boosted by the following reaction (58, 59, 106, 126):

$$M + H_3O^+ \rightarrow M^+ + H_2O + H$$

However, in the secondary reaction zone of hydrogen flames, hydrocarbon diluents do not affect alkali ionization, which is consistent with reaction (III. 7) (58, 76, 106, 126).

$$\text{(III. 7)} \quad M + X \rightleftarrows M^+ + e^- + X$$

The ionization of gallium, indium, and thallium is consistent with reaction (III. 7) too (78). The apparent collisional cross sections associated with reaction (III. 7) that are calculated from kinetic theory exceed the expected cross section values by several orders magnitude (76, 78). However, the calculated cross sections are considerably lower if ionization from electronically excited atomic states is considered (68).

The ionization of alkaline earth metals in O_2-N_2-H_2 flames appears to follow a different mechanism than the one consistent with alkali ionization (116). Most alkaline earth metals possess ionization energies that exceed those of the alkalis; however, alkali metals provide fewer ions.

The following mechanism for strontium ionization is consistent with experimental data (116):

$$Sr + OH \rightleftarrows SrOH^+ + e^-$$

or: $$SrO + H \rightleftarrows SrOH^+ + e^-$$

followed by : $$SrOH^+ + H \rightleftarrows Sr^+ + H_2O$$

The ionization work of Sugden and co-workers can be summarized by stating that the ionization of alkali metals results from energy transfer from a predominant flame species such as N_2 or H_2O in the secondary reaction zone of O_2-N_2-H_2 flames whereas charge transfer from a natural flame chemi-ion may occur in the primary reaction zone. Alkali metals apparently are not over-ionized in hydrogen flames; equilibrium ionization is approached from the under-equilibrium ionization side with the ionization rates for the various alkalis decreasing in the order Cs >K >Na >Li.

Hofmann and Kohn (64, 65) concluded that several alkali and alkaline earth metals were thermally ionized in air-C_2H_2 and air-N_2O-C_2H_2 flames.

Alkemade (2) originally favored the thermal mechanism of metal ionization in flames; however, a more thorough analysis of alkali ionization in O_2-N_2-CO flames led to a reconsideration. The important observations concerning alkali ionization in O_2-N_2-CO flames are as follows (68, 69): The ionization and recombination processes were

thermally equilibrated several centimeters downstream of the primary reaction zone; the transfer of vibrational energy from CO_2 and N_2 accounted for the ionization. However, above 30 mm in the O_2-N_2-CO flame, the temperature decreased rapidly with height, and the recombination reaction was too slow to follow the equilibrium amount of ionization exactly. The lag in the ion-electron recombination was manifested as supra-thermal ionization. Alkali ionization near the primary reaction zone appeared to be infra-thermal although some chemi-ionization was occurring. The rate of Saha ionization attainment for the various alkalis decreased in the order Cs > K > Na.

The various reports regarding the question of equilibrium metal ionization in flames are not consistent in their final conclusions. This apparent uncertainty prompted an experimental investigation of metal ionization in the N_2O-C_2H_2 flame, which hitherto has not been employed for such a study. The fact that the proponents of non-thermal metal ionization in flames performed their experiments in low temperature flames (temp $<2400\ ^{o}K$) is worthy to note. The higher gas temperatures attainable in the N_2O-C_2H_2 flame (temp $\sim 2900\ ^{o}K$) favor higher effective collision rates; metal ionization in the N_2O-C_2H_2 flame may be remarkably different from the non-thermal metal ionization observed in low temperature flames. The following investigation also provided an

opportunity to test several new methods for determining experimental ionization constants and clean flame electron pressures.

An experimental study of metal additive ionization in the nitrous oxide-acetylene flame

Experimental facilities and procedures The slot burner and accompanying spectrometric apparatus employed for this investigation were discussed in Chapter II. The gas flows into the burner were set to provide a fuel-rich flame with an unburnt acetylene to nitrous oxide mole ratio of 0.65; the flame was not luminous at this mixture strength. The premixed flame was characterized by a primary reaction zone extending only a few millimeters beyond the burner nozzle and a secondary reaction zone visibly extending a few decimeters. No photometric measurements were made in the primary reaction zone. The secondary reaction zone, which is a stable region of the flame, is suitable for making photometric measurements. When the $N_2O-C_2H_2$ flame is operated under fuel-rich conditions (i.e., $C_2H_2:N_2O = 0.65$), the secondary reaction zone is characterized by a red-colored zone extending for about two centimeters above the primary reaction zone. The red-colored zone is a highly reducing region of the flame; metal monoxide and hydroxide molecules exist only in reduced amounts in this interconal zone (25).

Aqueous solutions of metal chloride salts were prepared from reagent grade chemicals. Halide anions do not complicate the ionization study since gaseous halogens possess relatively low electron affinities (37, p. 116).

The flame gas rise velocity, which is cited in Figure 21, was determined by high speed cinematography. A fine aluminum powder was introduced into the flame through the pneumatic nebulizer. The hot, incandescent Al particles were tracked through the flame with a high speed motion picture camera (Fastax, model WF-3, Wollensak Optical Co., Rochester, N. Y.) operating at approximately 4000 frames per second.

Experimental approach The experimental approach employed to investigate metal ionization centers primarily about the following single equation:

$$K_{exp} = [M^+] [e^-]/[M^o]$$

The constant, K_{exp}, which describes the steady-state ionization-recombination balance between the metal atoms, metal ions, and electrons, is not a representation of the equilibrium ionization constant, K_S. An account of the experimental methods, which will be presented later, indicates that K_{exp} values for a particular metal can be determined by measuring the absolute number density and fractional ionization of the metal atoms in the flame. Deviations between the observed metal ionization and equilibrium

ionization will be determined by comparing K_{exp} values with K_{Saha} values, which are calculable by applying the measured flame temperature to equation (III. 6). If the reactants in the ionization-recombination steps are in local thermodynamic equilibrium, and if the rates of these two steps are large relative to the transit velocity of the metal through the flame, K_{exp} will necessarily equal K_{Saha}. Any observed deviations of K_{exp} from K_{Saha} must then be ascribed to either finite ionization-recombination rates or disequilibrium in the reactions or both (68, 69). Chemi-ionization is a non-equilibrium reaction.

Determination of flame temperatures The sensitivity of Saha ionization constants to the flame temperature requires that the ionization investigations be conducted in a flame region that can be characterized by a uniform, accurate temperature. The slot burner, flame, and experimental approach described herein fulfill these requirements to a high degree. The effects of vertical and lateral temperature gradients in the flame can be minimized by allowing the photometric detector to sample a narrow beam of radiation that focuses to an area 1 mm x 0.05 mm at the center of the burner slot. The effects of temperature gradients near the ends of the observed path length can be minimized by viewing the long-path, slot-burner flame end-on. The slot burner employed herein provides a longer slot than

most commercial slot burners. The importance of end effects can be tested by making line reversal temperature measurements as a function of indicator-element concentration (124).

All temperature measurements were made by applying the spectral line reversal technique, a convenient and commonly employed method (50, p. 234). The apparatus used to perform the line reversals has been described (136). The principle of the line reversal method is discussed theoretically and described practically in Appendix A.

The results of the line reversal temperature measurements appear in Table 6.

Table 6. Line reversal temperatures for the fuel-rich N_2O-C_2H_2 flame

Indicator element (resonance line)	Concn of element, μg/ml	Temp (°K) determined at 10 mm	20 mm	30 mm	40 mm
Ca (λ = 4227 Å)	1000	2890	2875	2840	2830
	500	2890	2875	2840	
	250		2875	2840	
Sr (λ = 4607 Å)	1000	2885	2880	2845	2830
	500	2885			
	250	2885			
Na (λ = 5889 Å)	1000	2860	2850	2815	2800
	500	2875	2860	2825	2815
	250	2885	2870	2835	2820
	100	2890	2880	2845	2830
Li (λ = 6708 Å)	1000	2855	2825	2800	2785
	500		2830		
	250		2870		
	100		2880		
	50		2880		

The reversal temperatures determined with the alkaline earths and low concentrations of the alkalis serving as indicators were in good agreement with one another. Evidently thermal equilibrium prevailed at the flame loci considered, at least up to a certain excitation energy. At high concentrations of the indicator-element, the flame becomes optically thick at the spectral regions of the emission lines, and the measured reversal temperatures favor the portion of the flame nearest the photometric detector. Since the temperatures measured with the alkaline earths serving as indicators were virtually invariant with respect to element concentration, the populations of free alkaline earth atoms were greatly reduced at the relatively cool ends of the slot burner flame. Free alkali atoms experienced minor variations in temperature at the ends of the flame since the alkalis indicated temperatures that deviated by a maximum of 50 ^{o}K to a minimum of zero ^{o}K from the temperatures indicated by the alkaline earth metals.

Determination of absolute number densities of free atoms Nearly all approaches to the evaluation of absolute number densities (N) of free atoms in flames lead to the determination of the $Nf_{o}l$ product. The absorption path length (l) can be measured easily; however, a literature value for the absolute oscillator strength (f_{o}) must be selected in order to derive a value for N. Two procedures,

which were employed for determining the $\underline{Nf_o l}$ product, are discussed below; relevant data for the elements selected for the ionization investigation are presented in Table 7.

Table 7. Selected properties of the metals included in the ionization study

Metal	Wavelength, Å	${}^{a}Q_a^e/g_1$	Oscillator strength Value	reference(s)
Ca	4227	1.00	1.60	(102)
Sr	4607	1.00	1.54	(104, 108)
Na	5889	1.00	0.66	(1)
Li	6708	1.00	0.75	(55, 72)

${}^{a}Q^e$ = electronic partition function = $\sum_j g_j \exp(-E_j/kT)$.

Fitting a theoretical curve of growth to an experimental curve of growth (73, 131) allows the determination of the $\underline{Nf_o l}$ product. This technique, which is described in detail in Appendix B, was employed to measure the number density of free calcium atoms in the flame.

The growth curves methods was not used for the determination of Sr, Na, and Li free atom number densities in the flame. In order to apply the growth curves method outlined in Appendix B, the spectral line of the element under study must be described by a single, symmetrical profile, which can be generated by the Voigt function. The Voigt function (Appendix B) does not present an accurate description of

the Li and Na resonance-line shapes since hyperfine structure components must be considered (131). Moreover, Li, Na, and Sr are ionized to a greater extent than Ca; this factor makes efficient ionization suppression more difficult, particularly at the relatively high metal concentrations required to produce the slope one-half regions of the growth curves.

A second method based on a continuum absorption technique was selected to determine absolute free-atom densities of Sr, Na, and Li. This method is described in Appendix C.

The results of the determinations of free atom absolute number densities are summarized in Table 8.

Table 8. Absolute free atom number densities for selected metals at an observation height of 20 mm in the N_2O-C_2H_2 flame

Metal[a]	Metal concentration in soln. μg/ml	rel. molarity x 10^{10}	N x 10^{-10}, cm^{-3}
Ca	1.0	.882	.882
Sr	1.0	.403	.392
Na	1.0	1.53	1.58
Li	0.5	2.54	1.57
Cu[b]	10	5.65	5.80

[a]Sufficient ionization buffer was present in each sample solution to efficiently suppress the ionization of the test species.

[b]For Cu 3247 Å, f_o = 0.34 (139).

In Table 8, the relative molarity of calcium was selected to be equal to the calcium free atom density. The relative molarities for the remaining four elements were calculated from their respective metal concentrations in solution and the relative molarity of calcium. The last two columns of Table 8 indicate that equimolar solutions of Ca, Sr, Na, and Cu yield equal number densities of free atoms, at least within the precision of the measurements and accuracy of the oscillator strength values. These observations strongly imply that the atomization of these four metals is complete (i.e., no compound formation occurs). Lithium does not follow the above mentioned trend for some inexplicable reason. Sodium (123) and copper (139) have previously been selected as reference standards denoting complete atomization.

Determination of fractional ionizations In the earlier discussion, the importance of the experimental determination of fractional ionizations was mentioned. The fractional ionization, α, of a gaseous metal in the flame is defined as follows:

$$\text{(III. 8)} \qquad \alpha = P(M^+)/P$$

$$\text{where:} \quad P = P(M^+) + P(M^o)$$

A common method of evaluating fractional ionizations is based on the ionization suppression technique: The

relative integrated atomic line intensity of a metal introduced into a flame is proportional to the number density of the free metal atoms if a correction for self-absorption is made. If an excess amount of a second metal with a low ionization energy is introduced into the flame, the ionization of the first metal is essentially quantitatively suppressed. The ionization suppression increases the relative integrated atomic line intensity of the first metal by an amount proportional to the initial free ion number density of the first metal. The fractional ionization of the first metal can be evaluated from the two relative line intensity measurements.

Compound formation in the flame could conceivably introduce an error into the ionization suppression technique for the determination of fractional ionizations. If free metal atoms participate in two competing quasi-equilibriums such as:

$$MX \overset{X}{\rightleftharpoons} M^{o} \rightleftharpoons M^{+} + e^{-}$$

suppression of the metal ion ($\underline{M}^{+}$) formation would not only produce more metal atoms ($\underline{M}^{o}$), but the amount of the stable compound (e.g. $\underline{MX}$) would increase too. Thus, the addition of an ionization buffer to a system such as the one above would increase the atomic line intensity of $\underline{M}^{o}$ by an amount that is not simply related to the original free metal ion

number density. However, compound formation for the metals studied herein appears to be negligible in the fuel-rich N_2O-C_2H_2 flame.

Experimental methods for the determination of K_{exp} and f Three different experimental methods were devised to determine K_{exp} values for metals in the N_2O-C_2H_2 flame. Two of the methods derive absolute values for K_{exp} and the clean flame electron pressure, f. A third method derives a K_{exp} value for one metal relative to a K_{exp} value for a second ionizable species.

The following equation provides the basis for all three of the experimental methods described herein:

$$(III.\ 9)\quad K_{exp} = P(M^+)\,[\,P(M^+) + f\,]/P(M^o)$$

where: $P(M^+)$ = partial pressure of metal ions,
= partial pressure of electrons contributed by the metal,
$P(M^o)$ = partial pressure of metal atoms,
and f = partial pressure of electrons contributed by the natural flame species.

In the application of (III. 9), f was assumed to be invariant with respect to metal additive at a given flame locus. This assumption has been made previously with some experimental justification (2, 68) and is consistent with the experimental

data presented later.

The first experimental method uses the fractional ionization relationship to good advantage. Substitution of (III. 8) into (III. 9) yields the following equation:

$$\text{(III. 10)} \quad \alpha P = K_{exp} (1-\alpha)/\alpha - f$$

The experimental evaluation of the absolute free-atom concentration (P) and fractional ionization (α) have previously been described. If α values are determined at various concentrations of the metal additive, sufficient information is obtained to plot αP on the ordinate versus $(1-\alpha)/\alpha$ on the abscissa, thereby yielding values for K_{exp} and f directly.

The second procedure is based on the quantitative evaluation of ionization interference effects, which have been discussed qualitatively in Chapter II. One variation of this method has previously been discussed (2). Basically, calculated ionization interference effects are compared with the experimental ionization interference effects. The "best" fit between the calculated results and the experimental results selects a value for f, which automatically fixes the K_{exp} value for the metal under study. The experimental ionization interference curves are obtainable by plotting relative integrated line emission intensities (corrected for self-absorption) as a function of

interferent concentration. The calculated ionization interference curves are evaluated at various $\underline{f}$ values as follows: The initial fractional ionization (no interferent present) and absolute free atom number density are experimentally determined for the element under study. These two quantities, along with a reasonable estimate for $\underline{f}$, are inserted into (III. 10) in order to fix the $\underline{K_{exp}}$ value. A modification of equation (III. 9) permits the calculation of the change in the fractional ionization of the metal under study (e.g., Ca, Sr) upon the addition of increasing amounts of an interferent (e.g., Cs, K), which increases the electron concentration in the flame. The calculated ionization interference curves are prepared by plotting the relative fractional ionization ($\underline{\alpha}$), or $\underline{1-\alpha}$ as the case may be, as a function of increasing interferent concentration.

This particular ionization interference method does not derive any basic information regarding the ionization nature of the interferent, which serves solely as a source of electrons whose absolute numbers are calculable. In principle, the ionization interference method can be employed to study alkali and alkaline earth metal ionization; however, the application of this method was restricted to the investigation of calcium and strontium ionization. With alkaline earth metals, ion lines as well as atom lines can be observed by flame spectroscopy. Since the calculated

ionization interference curves predict changes in free-atom number densities as well as free-ion number densities as a function of increasing interferent, the curve matching procedure can consider relative changes in free atoms and free ions. Thus, for the alkaline earths, each f value leads to two dependent calculated ionization interference curves, which must simultaneously fit two experimental curves.

The third method allows for the determination of K_{exp} for one metal relative to K_{exp} for a second metal. If a solution containing two ionizable metals is sampled and introduced into the flame, the two pseudo-equilibrium constants that describe the ionization are given as follows:

$$(III.\ 11)\quad K_{exp,1} = P(M_1^+)[\ P(M_1^+) + P(M_2^+) + f] \,/\, P(M_1^o)$$

$$(III.\ 12)\quad K_{exp,2} = P(M_2^+)[\ P(M_1^+) + P(M_2^+) + f] \,/\, P(M_2^o)$$

Ratioing (III. 11, 12) and retaining the definition of α:

$$(III.\ 13)\quad \frac{K_{exp,2}}{K_{exp,1}} = \left[\ \frac{\alpha_2}{1-\alpha_2}\ \right]\left[\ \frac{1-\alpha_1}{\alpha_1}\ \right]$$

Only two fractional ionization values must be measured to apply (III. 13) since the ratio of the K_{exp} values is independent of the amounts of the metals in the flame.

Results and Discussion The experimental ionization constants, which were determined for Ca, Sr, Na, and Li, have been compared with the Saha ionization constants, and reasonable explanations are presented to account for the deviations between the observed ionization and equilibrium ionization. The clean flame electron pressures are discussed in terms of absolute numbers, and the decay in f as a function of time is compared with relevant information in the literature.

Experimental values for K_{exp} and f The fractional ionization plots (αP vs. $(1-\alpha)/\alpha$) for the determination of K_{exp} and f for calcium and strontium are shown in Figures 15 and 16. Observations of the ionization of Ca and Sr were not made at heights greater than 20 mm above the burner since experimental evidence suggested that significant compound formation occurred beyond this point. Although there is considerable scatter of the experimental points in the calcium curves (Figure 15), least squares treatments of the data from replicate experiments provided K_{exp} and f values that deviated by only 10 per cent. For the calcium and strontium data, the linearity of the curves confirms that f indeed may be considered constant, irrespective of the metal additive concentration. The results obtained by applying the fractional ionization method are listed in Table 9.

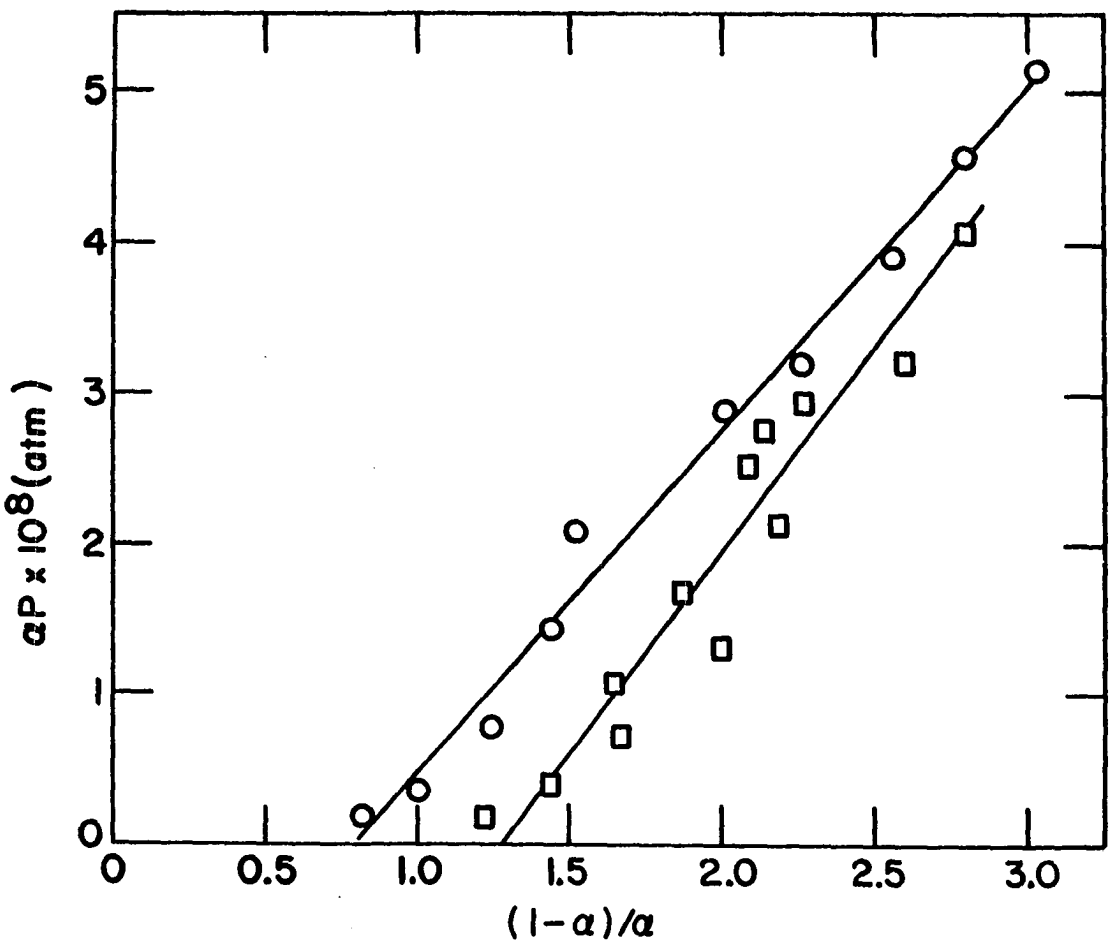

Figure 15. αP plots for calcium at observation heights of 20 mm (○) and 10 mm (□)

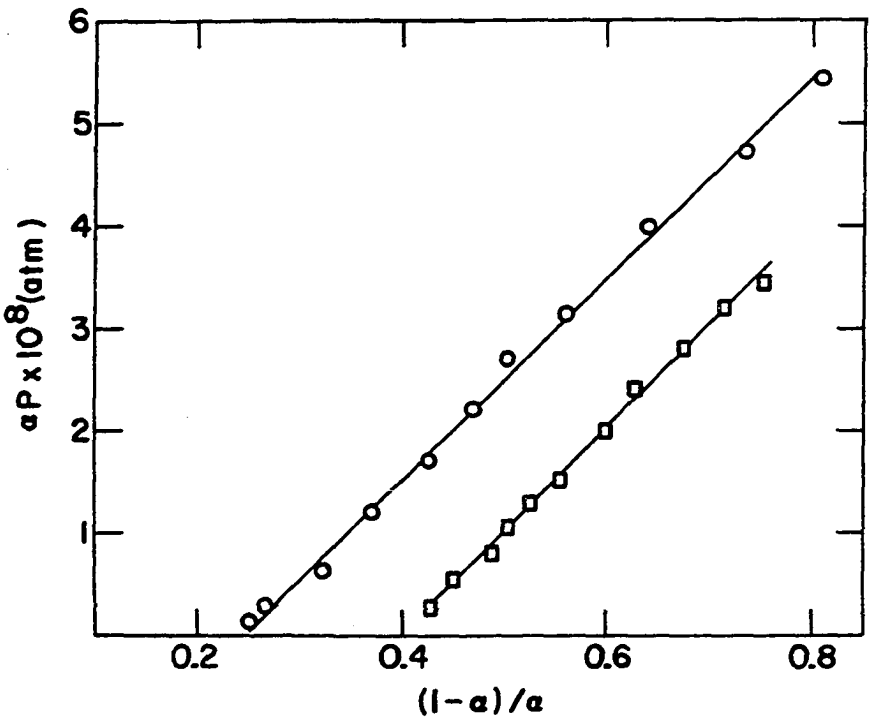

Figure 16. $\frac{\alpha P}{}$ plots for strontium at observation heights of 20 mm (O) and 10 mm (□)

Table 9. Experimental ionization constants for Ca, Sr, and Li and clean flame electron pressures in the N_2O-C_2H_2 flame

Method	Observation height (mm)	Ionization buffer or interferent	K_{exp} x 10^7 (atm)			$\underline{f}$ x 10^7 (atm)		
			Ca	Sr	Li	Ca	Sr	Li
fractional ionization	10	K	.27	1.0		.34	.37	
ionization interference	10	K	.26			.35		
	10	Cs	.26	.97		.35	.35	
fractional ionization	20	K	.23	.96	.49	.19	.23	.21
ionization interference	20	Cs	.24	.95		.23	.23	
	20	K	.24			.23		
	20[a]	K	.23			.22		
	20[b]	K	.23			.21		
fractional ionization	30	K			.38			.14
	40	K			.31			.10

[a]The calcium concentration was 10 μg/ml.

[b]The calcium concentration was 25 μg/ml.

Typical calculated and experimental ionization interference curves used to derive information on the ionization of calcium and strontium appear in Figures 17-20. The results obtained by applying the ionization interference method are listed in Table 9; the solution concentration of the metal under study was 5 μg metal/ml unless noted otherwise. In this group of figures, the calculated curves are based on $\underline{f}$ values differing by about 20 per cent. The ionization interference method is not extremely sensitive to changes in the $\underline{f}$ value; however, the sensitivity is improved for small concentrations of the element under study. Figures 17 through 20 along with the information presented in Table 9 lead to the following conclusions: The $\underline{f}$ values are reassuringly independent of the element under investigation. The $\underline{K_{exp}}$ and $\underline{f}$ values derived for calcium appear to be independent of the calcium concentration; evidently the assumption of a constant $\underline{f}$ is valid. The choice of the interferent (Cs or K) is not critical; this indicates that the evaluation of the electron number density generated by the interferent is accurate. The decrease in $\underline{f}$ as a function of increasing observation height is in harmony with the information presented in the earlier discussion of natural flame species ionization.

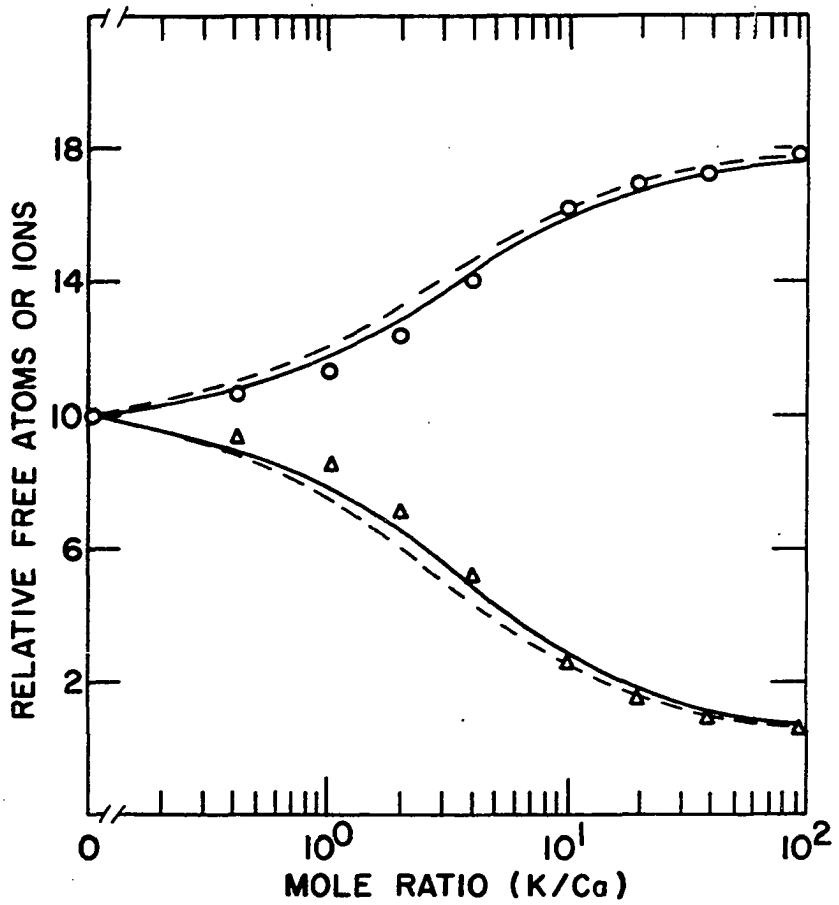

Figure 17. Ionization interference for K on Ca at an observation height of 20 mm. Experimental: relative Ca^o (O) and relative Ca^+ (Δ). Calculated: $\underline{f} = 0.22 \times 10^{-7}$ atm (——) and $\underline{f} = 0.18 \times 10^{-7}$ atm (---)

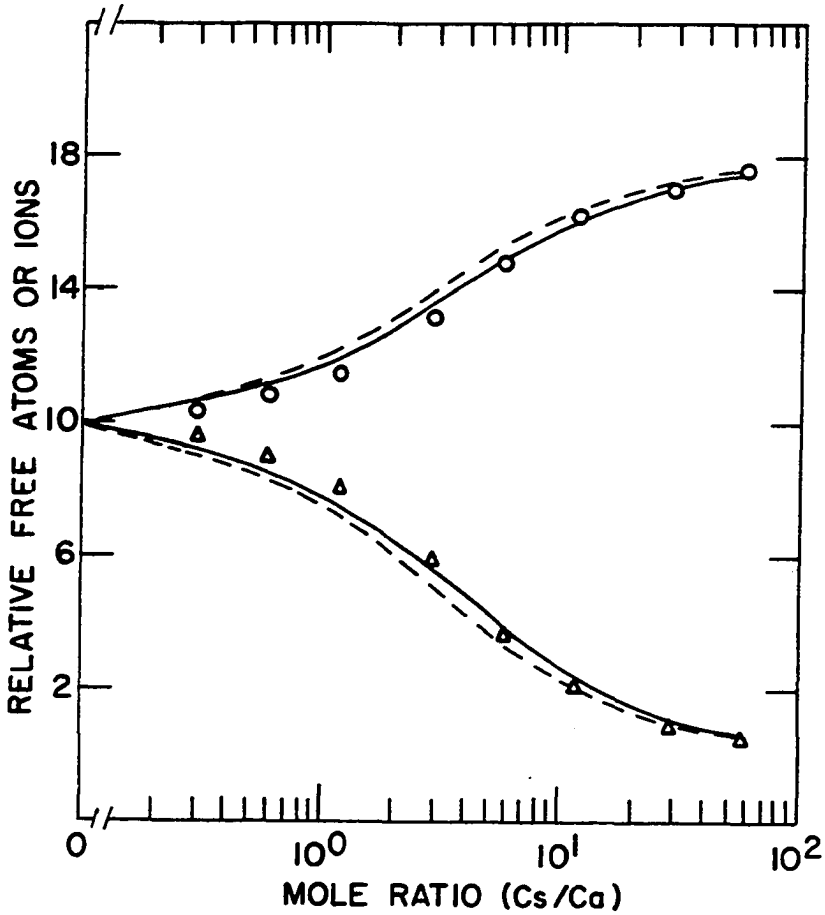

Figure 18. Ionization interference for Cs on Ca at an observation height of 20 mm. Experimental: relative Ca^0 (O) and relative Ca^+ (Δ). Calculated: $\underline{f}$ = 0.22 x 10^{-7} atm (——) and $\underline{f}$ = 0.18 x 10^{-7} atm (---)

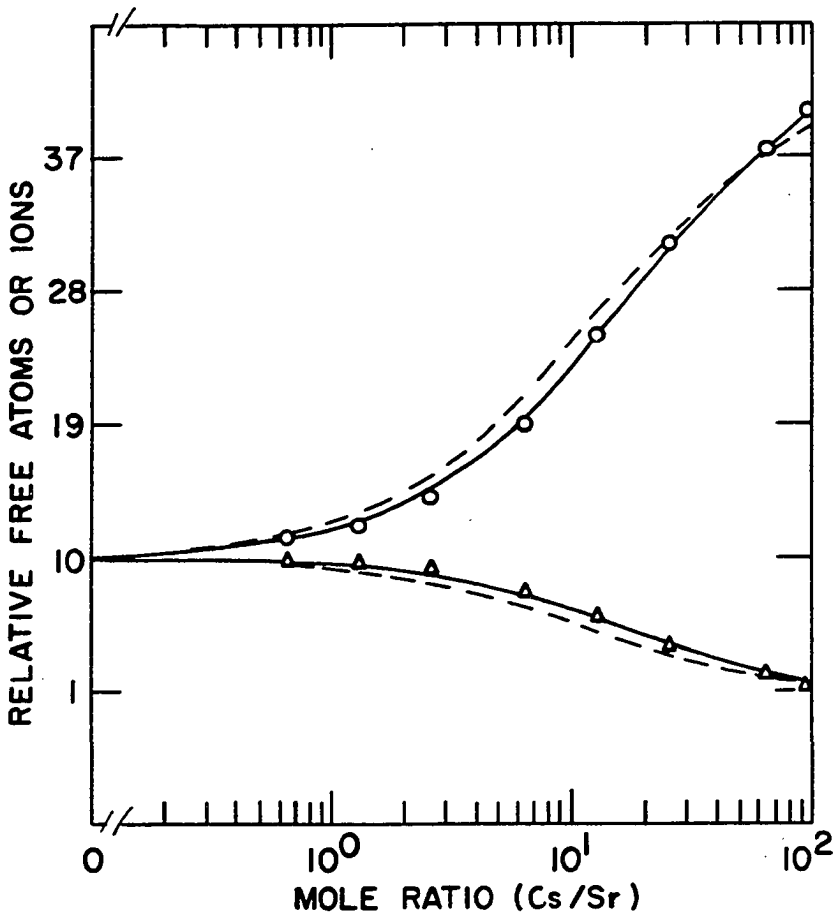

Figure 19. Ionization interference for Cs on Sr at an observation height of 20 mm. Experimental: relative Sr^0 (O) and relative Sr^+ (Δ). Calculated: $\underline{f} = 0.22 \times 10^{-7}$ atm (——) and $\underline{f} = 0.18 \times 10^{-7}$ atm (---)

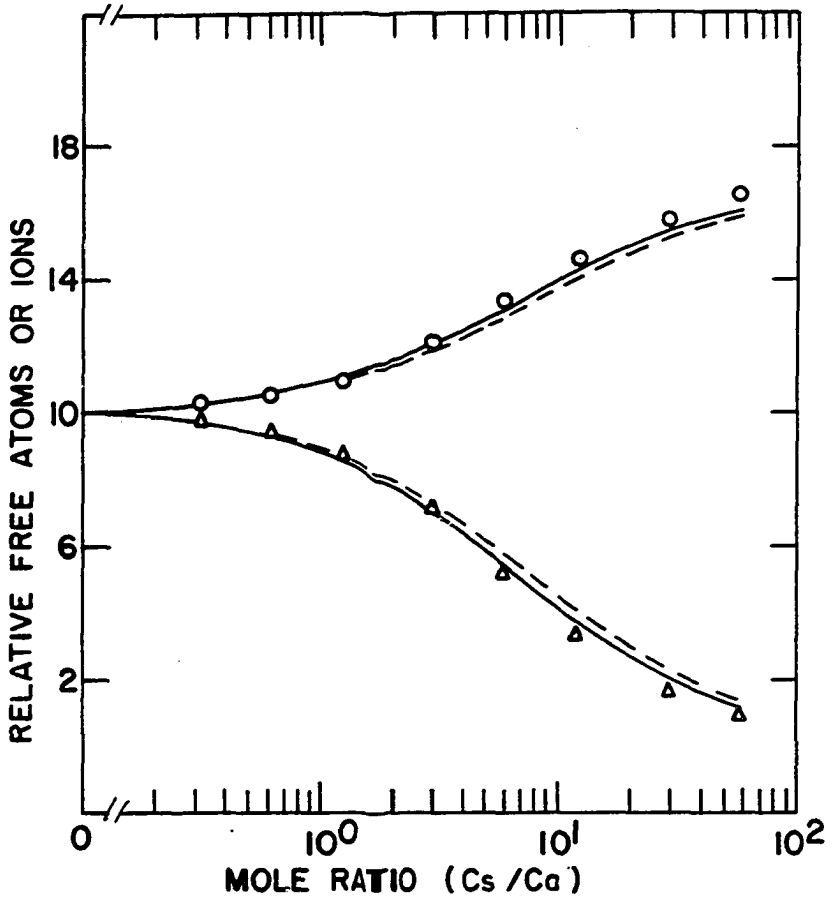

Figure 20. Ionization interference for Cs on Ca at an observation height of 10 mm. Experimental: relative Ca^0 (O) and relative Ca^+ (Δ). Calculated: $\underline{f}$ = 0.35 x 10^{-7} atm (——) and $\underline{f}$ = 0.41 x 10^{-7} atm (---)

For the determination of $\underline{K_{exp}}$ ratios via equation (III. 13), four different combinations of metal concentrations were chosen. The $\underline{K_{exp}}$ ratios from the ratio method, which are listed in Table 10, represent the average of four determinations, which deviated by approximately 10-15%. The good agreement between the ratios obtained via (III. 13)

Table 10. $\underline{K_{exp}}$ ratios for selected metals in the N_2O-C_2H_2 flame

$\underline{K_{exp}}$ ( )/$\underline{K_{exp}}$ ( ) ratio	Ratios from $\underline{K_{exp}}$ ratio method and (ratios from Table 9) at			
	10mm	20mm	30mm	40mm
Sr/Ca	3.6 (3.7)	4.3 (4.1)		
Li/Ca	1.3	2.2 (2.1)		
Li/Sr	.36	.49 (.51)		
Na/Ca	5.6	10.4		
Na/Sr	1.5	2.3		
Na/Li		5.2	4.7	4.6

and those obtained from the information in Table 9 is apparent by inspection. The ratios in Table 10 are also internally consistent. For example, the Li/Ca:Li/Sr quotients agree favorably with the Sr/Ca ratios.

Comparison of K_{exp} and K_{Saha} The focal question now is this: Are the K_{exp} values listed in Tables 9 and 10 in harmony with the equilibrium ionization constants that were calculated by inserting the line reversal temperatures into equation (III. 6)? The answer is provided by the information presented in Figure 21; however, before this figure can be properly interpreted, several precautionary comments are in order. High in the flame, the K_{exp}/K_{Saha} curve for Li should approach unity from above the unit level if the results in Figure 21 are to be consistent with previously established facts (see discussion on page 74 and (68, 69)). Although the cause of the slight disposition of the $K_{exp}(Li)/K_{Saha}$ curve has not been unequivocally identified, several sources of error in the experimental measurements can readily account for a vertical adjustment on the K_{exp}/K_{Saha} axis. A ten per cent error in the determination of the K_{exp} values is very reasonable. The accuracy of the temperatures is approximately ten kelvins, and Saha constants change approximately one per cent for each degree of temperature change.

In Figure 21, the position of the Li and Na points at 10 mm indicates that Na reaches thermal ionization more rapidly than Li. The rates at which alkali metals reach Saha ionization have previously been reported to decrease in the order Cs> K> Na> Li (86) in air-H_2 flames and in

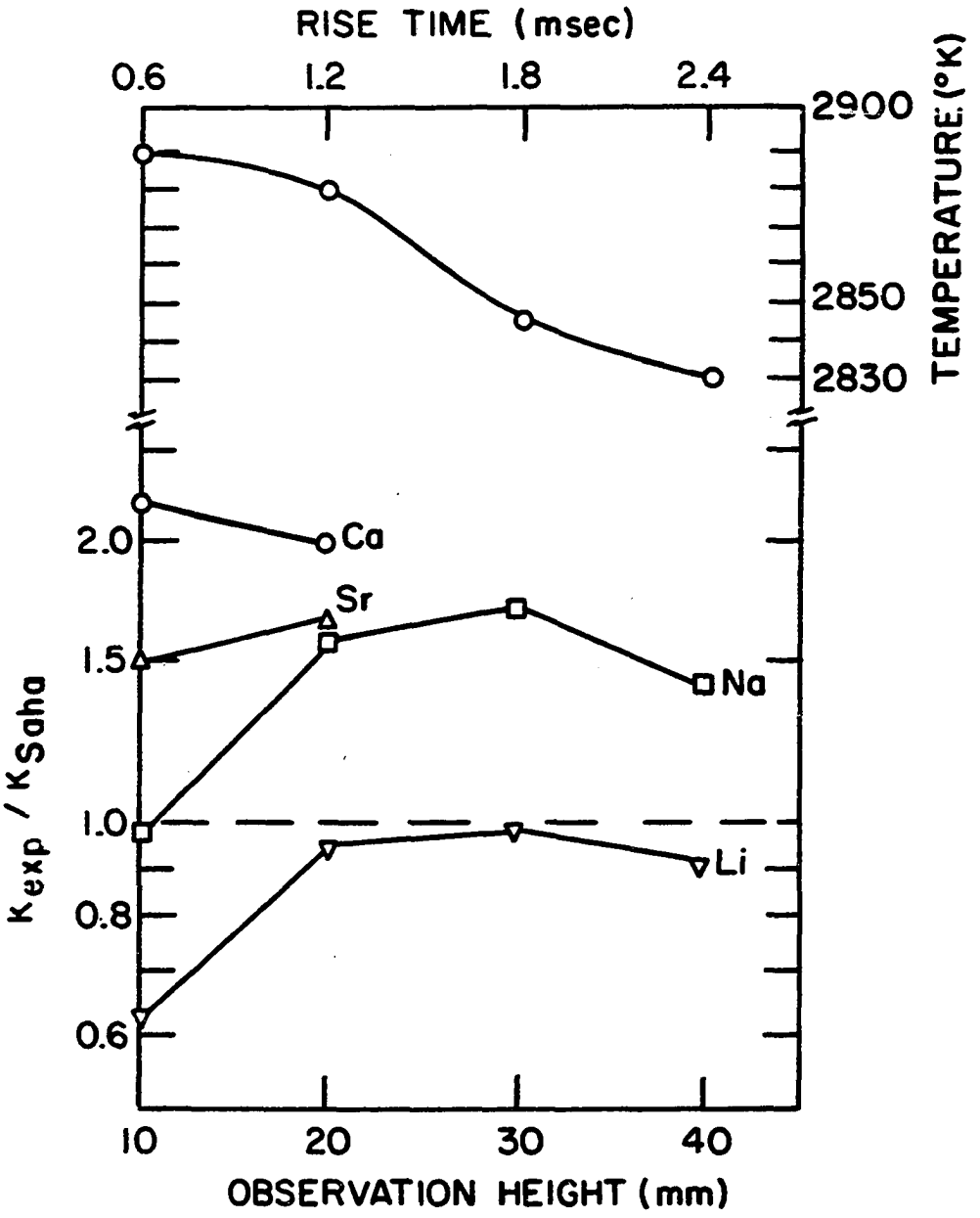

Figure 21. Comparison of $\underline{K_{exp}}$ values with $\underline{K_{Saha}}$ values at various observation heights. Vertical temperature profile

the order Cs > K > Na (68, 69) in air-CO flames. The high $\underline{K_{exp}}(Na)/\underline{K_{Saha}}$ value at 20 mm must result from some chemi-ionization process since $\underline{K_{Saha}}$ decreases only ten per cent from 10 mm to 20 mm. At observation heights exceeding 20 mm, chemi-ionization must become less important, and at heights of 30 mm and 40 mm, $\underline{K_{exp}}/\underline{K_{Saha}}$ values exceed unity because of the slow rates of the ion-electron recombination processes relative to rate at which Saha constants change as a function of the decreasing temperature. The recombination rates of alkali ions and electrons decrease in the order Li > Na > K > Rb > Cs (80) and are approximately two orders of magnitude smaller than the recombination rate of natural flame chemi-ions and electrons.

The observations that the ionization behavior of calcium and strontium departs significantly from the behavior of the alkali ionization can be reconciled by considering chemi-processes, which become increasingly important relative to thermal processes for reactions characterized by high activation energies (51). If the energy released in the chemical rearrangement of the reactants exceeds the ionization energy of the metal atom, chemi-ionization, which is virtually insensitive to the metal ionization energy, can occur. Several plausible chemi-ionization reactions are listed below. In contrast, however, thermal ionization rates decrease exponentially with increasing metal ionization

energies. The observation that calcium, which has an ionization energy of 6.12 eV, exhibits greater supra-thermal ionization than strontium, which has an ionization energy of 5.70 eV, is also in harmony with this interpretation. The alkaline earth ionization mechanism (116) previously discussed on page 73 should not be applicable in the N_2O-C_2H_2 flame since the chemical environment is not favorable for the existence of the species MO, MOH, and MOH^+.

The rationale behind the production of supra-thermal amounts of metal ions by chemi-ionization may be explained by considering the following example: In the O_2-N_2-CO premixed flame, supra-equilibrium amounts of flame radicals (i.e., CO, O) are known to exist in the primary reaction zone and persist for a few milliseconds beyond this zone (68, 69). The reaction schemes (III, 14, 15) can account for chemi-ionization of the metal, M (68, 69).

(III. 14) $CO + O + M \rightleftarrows CO_2 + M^+ + e^-$

(III. 15) $CO + O + X \rightleftarrows CO_2 + X^*$

$M + X^* \rightleftarrows M^+ + e^- + X$

where X^* is a supra-thermally excited third body

The CO_2 species in the above reactions is a major constituent of the flame gases and is not significantly affected in amount by changes in the concentrations of CO and O, which are minor constituents (5). Consequently, the ion-electron recombination processes outlined in (III. 14, 15) would tend to create equilibrium numbers of the metal atom, whereas the ionization reactions would necessarily lead to supra-thermal amounts of metal ions. Therefore, chemi-ionization processes lead to a steady-state balance between reactants and products rather than the establishment of Saha equilibrium.

The data collected in the present study do not provide definitive bases for identifying the exact mechanisms leading to chemi-ionization of metal additives in flames. Chemi- processes are particularly difficult to identify in complex hydrocarbon flames. Gaydon and Wolfhard point out that abnormally high excitation and ionization in flames may be related (50, p. 323; 51). The similarities in the experimental conditions that lead to chemi-ionization and chemiluminescence suggest a close relationship between these two phenomena. For example, a direct proportionality exists between the effectiveness of chemi-ionization and chemi-excitation and the energy associated with the complete oxidation of the carbon in the fuel (15). The predominantly thermal nature of excitation and ionization in O_2-H_2 and O_2-CO flames along with the commonly observed chemi-excitation

and chemi-ionization of natural flame species and metal additives in hydrocarbon flames further suggests a close relationship between the two chemi-processes (15, 17, 22, 79, 128). Several reactions, which provide sufficient energy for the observed chemi-processes, have been postulated. Broida and Shuler (14) suggest the following chemi-excitation process, which closely resembles mechanism (III. 1) for primary chemi-ion formation:

$$\text{(III. 16)} \quad CH(CH_2) + O + M \rightarrow CO + H(H_2) + M^*$$

However, reaction (III. 16) is not entirely consistent with all experimental information (17, 51). The supra-thermally excited species, whether it be M^* or an intermediate such as X^*, should be produced by a bimolecular reaction such as:

$$\text{(III. 17)} \quad CH + O \rightarrow CHO^* \qquad (18)$$

$$\text{or (III. 18)} \quad CH + O \rightarrow CO^* + H \qquad (15)$$

The active species in (III. 17, 18) could be responsible for either chemi-ionization or chemi-excitation of a metal additive. The very strong parallel between chemi-ionization and chemi-excitation of metal additives has also led to the postulation of the following mechanisms:

$$\text{(III. 19)} \quad CH + O + M \rightarrow CO + H + M^+ + e^- \quad (17)$$

$$\text{and (III. 20)} \quad R^+ + M \rightarrow M^+ + e^- + R \qquad (17, 22, 106)$$

where R^+ is a natural flame species chemi-ion. In order for chemi-excitation of metal atoms to accompany reactions (III. 19, 20), the following two-body reaction assumedly occurs (17):

$$M^+ + e^- \rightarrow M^*$$

The preceding listing of chemi-reactions merely points out several suggested mechanisms, which can lead to chemi-ionization and chemi-excitation. However, fuel-rich hydrocarbon flames generally produce small concentrations of radicals in the primary reaction zone (44, 75). In the post primary reaction zones of flames containing excess hydrocarbons, flame radicals allegedly recombine via fast bimolecular reactions rather than the more common, slower termolecular processes (44). The apparent lack of supra-thermal quantities of flame radicals beyond the primary reaction zone suggests an explanation for the observed confinement of chemi-luminescence of metal additives to the primary reaction zone of hydrocarbon flames (17, 51). The observation of supra-thermal amounts of metal ions in the secondary reaction zones of hydrocarbon flames (17, 80, 128) does not suggest a major break in the similarities between chemi-ionization and chemi-excitation. The recombination of metal ions and electrons is much slower than the quenching of electronically excited species. Thus, supra-thermal quantities of metal ions formed in the primary reaction zone

of a hydrocarbon flame may extend well into the secondary reaction zone as equilibrium amounts of these species are being established. However, if chemi-ionization of metal additives does indeed occur in the secondary reaction zone of a fuel-rich hydrocarbon flame, reaction (III. 20) is a likely mechanism since natural flame chemi-ions are known to persist in this region (85).

Clean flame electrons The clean flame electron pressures and number densities listed in Table 8 and Figure 22 are in reasonable agreement with typical values reported in the literature (2, 112, 119). The presentation of clean flame electrons in Figure 22 suggests that a second order recombination process accounts for the electron removal. A reaction such as:

$$R^+ + e^- \xrightarrow{k_r} \text{products}$$

where $P(R^+) = P(e^-)$, is consistent with Figure 22 and the previous discussion of natural chemi-ion-electron recombination, which considered:

$$\text{(III. 4)} \quad H_3O^+ + e^- \xrightarrow{k_r} \text{products}$$

The H_3O^+ ion is indeed the dominant ion downstream from the primary reaction zone in nearly stoichiometric acetylene flames. The measured recombination coefficient, k_r, for reaction (III. 4) is 2×10^{-7} cm^3 sec^{-1} (20, 94). The slope

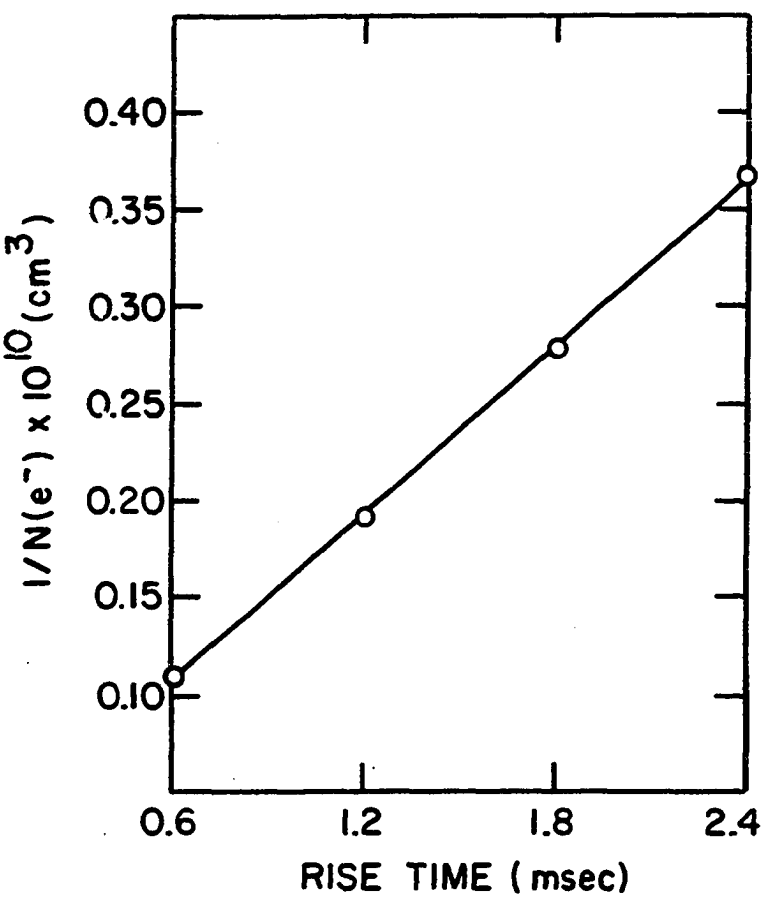

Figure 22. Time-decay of the "clean" flame electrons

from the curve in Figure 22 indicates a recombination coefficient of 2×10^{-8} cm^3 sec^{-1}. The apparent disagreement in the recombination coefficients can be reconciled by recalling that the predominant chemi-ion in the secondary reaction zone of a fuel-rich acetylene flame bordering on luminosity is not H_3O^+ but rather is $C_3H_3^+$ (85). Although the number density of chemi-ions in a fuel-rich flame is generally reduced from the number density in a nearly stoichiometric flame, the chemi-ions persist approximately ten times longer in the former flame (85). Thus, the apparent chemi-ion-electron recombination lag in the fuel-rich flame can readily account for the difference between the typical literature values for $\underline{k_r}$ and the value derived herein.

Appendix A

The line reversal method for temperature determinations

A line reversal temperature is one quantity that describes the population of excited states. If the Boltzmann equation holds in a small flame volume characterized by a single translational temperature, the reversal temperature will equal the translational or "true" temperature in this region. However, the slight amount of radiative disequilibrium present in all conventional flame systems does account for deviations from the Boltzmann equation. Fortunately, most hydrocarbon flames are blessed with an abundance of molecules capable of efficiently quenching electronically excited states. Efficient collisional deactivation reduces the effects of radiative disequilibrium on the Boltzmann equation so that population temperatures in hydrocarbon flames approach translational temperatures within a few kelvins (124).

The theoretical basis for the reversal technique can be outlined in the following way. The integrated emission intensity of a spectral line is given by:

(A. 1) $$\int_{\text{line}} I_{em}(\nu)d\nu = I_{\nu_o}^{bb}(T_f) \int_{\text{line}} (1-e^{-k(\nu)l})d\nu \quad (95)$$

where: $I_{\nu_o}^{bb}(T_f)$ = intensity of a blackbody at frequency ν_o and flame temperature $^{o}T_f$ (^{o}K)

ν_o = peak frequency of the spectral line; $k(\nu)$ = absorption coefficient and l = absorption path length

For the line intensity in an optically thin source, (A. 1) reduces to:

$$(A.\ 2)\qquad \int_{line} I_{em}(\nu)d\nu = I^{bb}_{\nu_o}(T_f) \int_{line} k(\nu)l\, d\nu$$

Since:

$$(A.\ 3)\qquad \int_{line} k(\nu)l\, d\nu = \frac{\pi e^2}{mc} N_l f_o l \qquad (95)$$

where: e = charge of the electron

m = mass of the electron

N_l = number density of atoms in the lower state

c = speed of light

f_o = oscillator strength for the transition

and:

$$(A.\ 4)\qquad \frac{g_u}{g_l}\frac{\lambda_o^2 A}{8\pi} = \frac{\pi e^2}{mc} f_o \qquad (95)$$

where: g_u, g_l = statistical weights of the upper and lower states

λ_o = wavelength of the transition and

A = Einstein transition probability

and:

$$(A.\ 5)\qquad I^{bb}_{\nu_o}(T_f) = \frac{8\pi h \nu_o^3}{c^2} e^{-\frac{h\nu_o}{kT_f}} \qquad (40)$$

where: h = Planck constant and k = Boltzmann constant

and:

$$(A.\ 6)\quad \frac{N_u}{N_l} = \frac{g_u}{g_l}\ e^{-\frac{h\nu_o}{kT_f}}$$

equations (A. 3-6) can be substituted into (A. 2) to arrive at the following standard equation for a spectral line when self-absorption is negligible (62):

$$\int_{line} I_{em}(\nu)d\nu = N_u A l h\nu_o$$

Note that equation (A. 5) is referred to as Wien's law. Wien's law, which is satisfactory for the blackbody distributions required herein, reduces to Planck's blackbody distribution for small values of $\underline{\lambda T}$.

Beer's law for light absorption states that:

$$(A.\ 7)\quad I_{tr}(\nu) = I^o(\nu)\ \exp(-k(\nu)l) \qquad (95)$$

where: I_{tr} = transmitted intensity and
I^o = incident intensity

From (A. 7), the integrated absorbed intensity is:

$$(A.\ 8)\quad \int_{line} I_{abs}(\nu)d\nu = I^o_{\nu_o} \int_{line} 1-e^{-k(\nu)l}\ d\nu$$

if the incident intensity is constant over the frequency range of the spectral line. The source of the incident intensity $\underline{(I^o_{\nu_o})}$ can be characterized by a brightness

temperature (T_b) at a particular radiation frequency (ν_o). The brightness temperature of a source is defined as the temperature at which a blackbody emits the same spectral intensity of radiation as the source (109). Thus, equation (A. 8) can be expressed as follows:

$$\text{(A. 9)} \qquad \int_{\text{line}} I_{abs}(\nu)d\nu = I^{bb}_{\nu_o}(T_b) \int_{\text{line}} 1-e^{-k(\nu)l}\, d\nu$$

Ratioing (A. 1) and (A. 9):

$$\text{(A. 10)} \qquad \frac{\int_{\text{line}} I_{em}(\nu)d\nu}{\int_{\text{line}} I_{abs}(\nu)d\nu} = \frac{I^{bb}_{\nu_o}(T_f)}{I^{bb}_{\nu_o}(T_b)}$$

In performing a line reversal, light from a primary source is focused on an emission source that in turn is focused on the entrance slit of a spectrometer. The emission source, a flame for the purposes herein, is generally salted with an indicator-metal that emits the spectral line used for the reversal. The primary source (Projection Lamp, type EDW-18A-6V, Westinghouse Electric Corp., Bloomfield, N.J.) is generally a tungsten strip and the electric current passed through the strip determines the intensity of the strip's radiation. The current through the tungsten ribbon is varied until the light emission from the flame is balanced with the light absorption from the primary source. At this point, the value of the ratio in (A. 10) becomes unity, and

the flame temperature equals the brightness temperature of the source.

An optical pyrometer (Automatic Optical Pyrometer, model 8641, Leeds and Northrup Co., Philadelphia, Pa.) was used to determine the brightness temperature of the tungsten source. Since the resonance wavelength of the spectral line usually differs from the peak wavelength of the pyrometer's spectral bandpass (6500 Å), the variation of tungsten emissivities with wavelength (32) must be considered in the evaluation of the flame temperature from the brightness temperature of the tungsten at 6500 Å.

Appendix B

The determination of Nf_o1 by the growth curves method

An experimental curve of growth is a double logarithmic plot of integrated emission (or absorption) intensity versus metal concentration in solution. The proportionality between integrated emission and integrated absorption can be seen by comparing (A. 1) and (A. 8). If a growth curve is constructed for a metal capable of forming ions, the intrinsic ionization of the metal must be quantitatively suppressed. The experimental growth curve for calcium (shown by the points in Figure 23) was derived by measuring the integrated emission intensity of the Ca(I) 4227 Å line as a function of the calcium solution concentration. Integrated emission (or a proportional quantity) can be determined by measuring the apparent peak emission intensity when certain conditions are fulfilled. If the mechanical slits of the monochromator are sufficiently large to keep the total slit function constant over the spectral region of the emission line, the peak intensity of the recorded output is indeed proportional to the integrated emission intensity (109). If the slit width is too small to meet this requirement, the experimental growth curve does not reach the theoretical limiting slope of one-half. Reaching the correct theoretical limiting slope is also reassuring from the standpoint that complete vaporization of the aerosol droplets and linearity

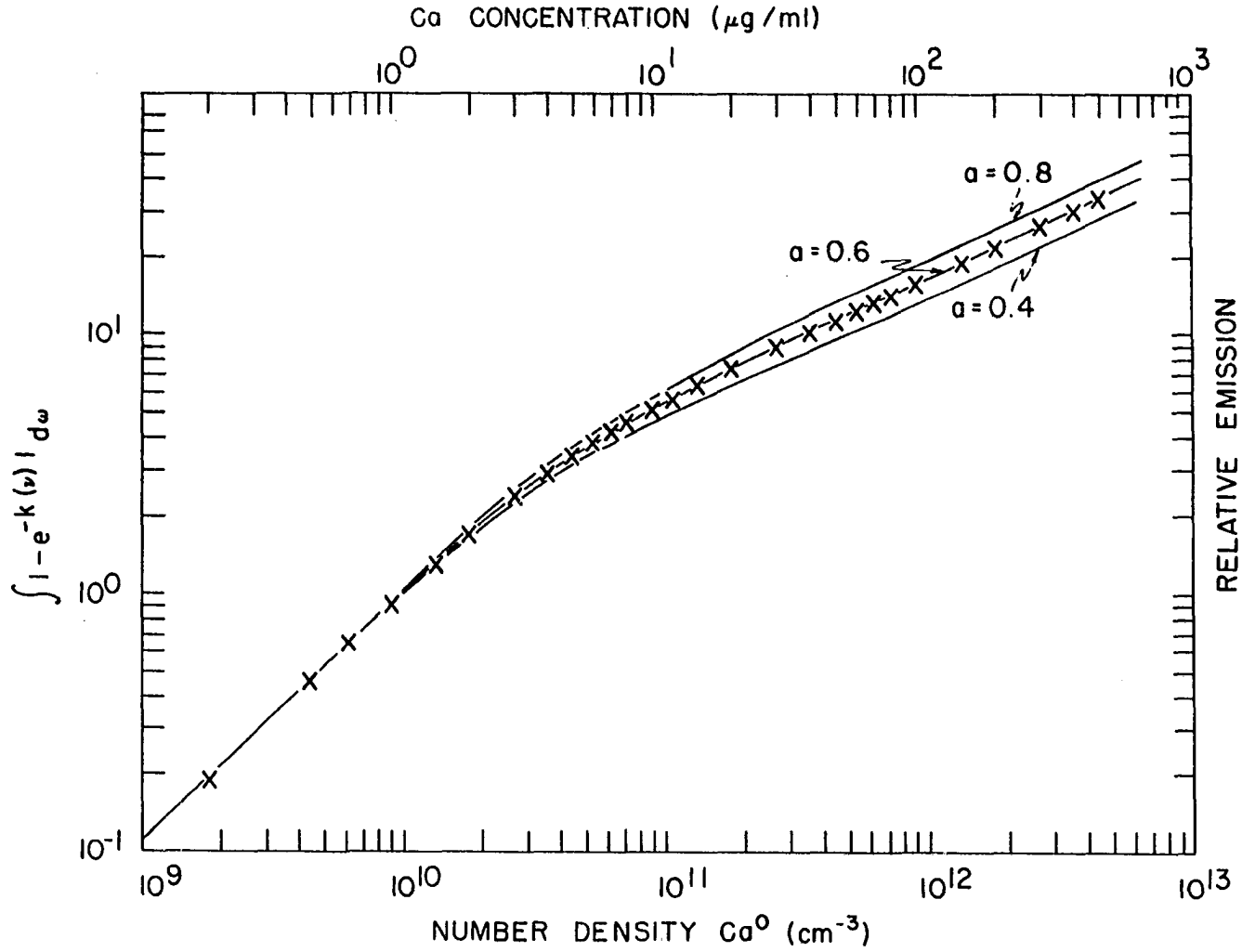

Figure 23. Theoretical and experimental curves of growth for calcium (λ = 4227 Å). Observation height = 20 mm

of aerosol production is implied.

Theoretical growth curves are constructed by evaluating the integrated absorptivity ($\int_{line} 1-e^{-k(\nu)l}d\nu$) and plotting this integral (or a proportional quantity) as a function of the $Nf_o l$ product or absolute number density if an oscillator strength value is selected from the literature. The proportionality between integrated emission (or absorption) and integrated absorptivity is evident from (A. 1, 8). The calcium solution concentration is also sensibly proportional to the number density of free calcium atoms in the flame. Therefore, it is reasonable to compare experimental and theoretical curves of growth on a double logarithmic plot.

The absorption coefficient ($k(\nu)$) or the "line shape" must be known to evaluate the integrated absorptivity. For isolated spectral lines that don't possess hyperfine or isotopic structure, Doppler broadening and collisional broadening predominate in the description of the absorption coefficient (4). For a spectral line broadened only by the Doppler effect, the absorption coefficient is:

$$(B.\ 1)\quad k(\nu)^{D} = \frac{2}{\Delta\nu_D}\sqrt{\frac{\ln 2}{\pi}}\,\frac{\pi e^2}{mc}\,N_1 f_o \exp-(2(\nu-\nu_o)\sqrt{\ln 2}/\Delta\nu_D)^2 \quad (95)$$

where: ν_o = frequency of line center and

$\Delta\nu_D$ = full width at half maximum (or half-width) for a pure Doppler line

$$\text{(B. 2)} \qquad = \sqrt{8kT\ln 2/Mc^2}\ \nu_o$$

where: M = mass of the emitter or absorber

Equation (B. 1) has been normalized to meet the requirement stated by (A. 3). The original theory of collisional or pressure broadening was treated by Lorentz in 1906 (95). Collisions reduce the lifetime of an excited state thereby leading to an increased half-width of the spectral line. The absorption coefficient for a pure Lorentzian spectral line is:

$$\text{(B. 3)} \qquad \overset{L}{k}(\nu) = \frac{2/\pi\Delta\nu_L}{1 + \left[\frac{2(\nu-\nu_o)}{\Delta\nu_L}\right]^2} \qquad (95)$$

where: $\Delta\nu_L$ = half-width for pure Lorentzian line

$$= \frac{1}{\pi\tau}$$

where: τ = mean life of excited species

Since $\underline{\overset{L}{k}(\nu)}$ and $\underline{\overset{D}{k}(\nu)}$ describe the total absorption coefficient, the pure Doppler distribution is convoluted with the Lorentzian distribution to generate the total absorption coefficient given by the following Voigt function:

$$(B.\ 5)\quad k(\nu) = \int_{-\infty}^{+\infty} \frac{\pi e^2}{mc} \frac{2}{\Delta\nu_D}\sqrt{\frac{\ln 2}{\pi}}\, N_1 f_o \exp-(2\sqrt{\ln 2}\, t/\ \Delta\nu_D)^2 \times \frac{2/\pi\Delta\nu_L}{1 + \left[\frac{2(\nu - \nu_o - t)}{\Delta\nu_L}\right]^2} dt$$

where: t = integration variable

By introducing:

$$y = \frac{2\sqrt{\ln 2}\, t}{\Delta\nu_D}$$

$$\omega = \frac{2(\nu - \nu_o)\sqrt{\ln 2}}{\Delta\nu_D}$$

$$(B.\ 6)\qquad a = \frac{\Delta\nu_L}{\Delta\nu_D}\sqrt{\ln 2} \quad \text{and}$$

$$k_o^D = \frac{2}{\Delta\nu_D}\sqrt{\frac{\ln 2}{\pi}}\,\frac{\pi e^2}{mc}\, N_1 f_o$$

equation (B. 5) reduces to:

$$(B.\ 7)\quad k(\nu) = k_o^D\, \frac{a}{\pi} \int_{-\infty}^{+\infty} \frac{\exp(-y^2)\, dy}{a^2 + (\omega - y)^2}$$

The integral in (B. 7) must be solved numerically; the method suggested by Rann (114) was used herein.

The cross sections for collisions between excited species and flame gas constituents vary as a function of the flame chemistry and generally are not known for many reactions. As a result, the Voigt function (B. 7) is evaluated as a

function of the a parameter. The theoretical curves appear as solid curves in Figure 23.

The growth curves are characterized by three distinct regions. The slope = 1 region prevails at low optical densities, i.e., when self-absorption is negligible. In this region the integrated absorptivity does not depend on the line shape. At extremely high optical densities, the slope = 1/2 region is attained. At intermediate values for the optical density, the transition regions between slopes 1 and 1/2 possess distinctly different curvatures for different a parameter values, thereby creating a region that allows the "best" fit between the experimental curve and one theoretical curve to be determined. The relationship between calcium solution concentration and number density calcium atoms in the flame can be determined from Figure 23.

An extra feature of the growth curve method is the evaluation of the a parameter. Since line half-widths for Doppler profiles can be calculated from (B. 2), the mean-life of the excited species between collisions can be determined by applying (B. 2) and (B. 4) as follows:

$$\frac{1}{\tau} = \frac{a \pi \Delta\nu_D}{\sqrt{\ln 2}}$$

Now, $1/\tau$ is the rate constant for collisional deactivation of the excited state of a certain species; similarly A is the

rate constant for radiational deactivation. A comparison of $\underline{1/\tau}$ with $\underline{A}$ for the particular calcium transition under consideration indicates that the collisional deactivation rate exceeds the radiational rate by a factor of approximately 100. This bit of evidence supports the claim that radiative disequilibrium does not significantly affect the Boltzmann equation in the N_2O-C_2H_2 flame.

Appendix C

The determination of $Nf_o l$ by a continuum absorption method

If the spectral region encompassing an absorption line is scanned by advancing the wavelength selector on the monochromator, the total area indicated as an absorption on the recorder tracing is proportional to the integrated absorptivity when a continuum serves as the primary source (109). Generally, these areas are measured by the rather tedious and irreproducible planimetering technique. An alternative, more convenient, continuum absorption technique was employed to measure the integrated absorptivity.

Since monochromators do not in general, possess very large resolving capabilities relative to spectral line widths, the concept of slit functions must be introduced. The total slit function:

$$s(|\nu' - \nu|)$$

essentially says that the instrument indicates some response at frequency ν' when it is set at frequency ν (109). If light from a continuum source illuminates the entrance slit of a monochromator, the photometric signal (P_1) proportional to:

$$\int_{\nu'} I^o \, s(|\nu' - \nu|) \, d\nu'$$

If the primary source radiation is passed through a flame salted with some analyte while the wavelength selector of the monochromator is peaked at the absorption frequency, the apparent absorbed intensity (P_2) becomes with the help of (A. 8):

$$P_2 \propto \int_{\nu'} I^o \, s(|\nu' - \nu|)\,[\,1 - e^{-k(\nu)l}\,]\,d\nu'$$

The fractional absorption (A_F) is defined as the ratio of P_2 to P_1:

$$(C.\ 1)\quad A_F = \frac{\int_{\nu'} I^o \, s(|\nu' - \nu|)\,[1 - e^{-k(\nu)l}]\,d\nu'}{\int_{\nu'} I^o \, s(|\nu' - \nu|)\,d\nu'}$$

Experimentally, the geometrical size of the entrance slit was set equal to the exit slit. Thus, $s(|\nu' - \nu|)$ is a triangular function (109, 118). Large entrance and exit slits on the monochromator were selected in order for the slit function to be essentially constant over the spectral region of absorption. Under these conditions, (C. 1) reduces to:

$$(C.\ 2)\quad A_F = \frac{\int_{\text{line}} 1 - e^{-k(\nu)l}\,d\nu}{\Delta\nu_B}$$

where: $\Delta\nu_B$ = half-width of slit function or spectral bandpass

If self-absorption is insignificant in the absorption cell, (C. 2) can be written as follows:

$$(C.\ 3)\quad \frac{\pi e^2}{mc}\ N_1 f_o l = A_F\ \Delta\nu_B$$

where A_F can be measured by the dc absorption technique (64). Usually $\Delta\nu_B$ is evaluated by multiplying the reciprocal linear dispersion of the monochromator by the geometric slit width (64). However, for a poorly adjusted instrument, this approach may introduce an error. The following technique was used to evaluate the spectral bandpass of the monochromator: From the calcium growth curves, the absolute absorptivity for Ca was known at many calcium solution concentrations. Measurement of A_F for a calcium sample and the application of (C. 2) allowed the determination of $\Delta\nu_B$ at the calcium resonance wavelength of 4227 Å. Since $\Delta\lambda_B$ is constant over a wide spectral range, $\Delta\nu_B$ values were calculated at the resonance wavelengths of Sr, Na, and Li. The free-atom number densities of Sr, Na, and Li were determined via (C. 3) after A_F values were measured for these three metals.

CHAPTER IV. SUMMARY

Chemical interferences commonly encountered in analytical flame spectroscopy were investigated in premixed flames of acetylene and air, oxygen, or nitrous oxide. Condensed-phase or solute-vaporization chemical interferences have been discussed at great lengths in the literature mainly because of their magnitude, persistence, and wide occurrence. The purpose of this research was to find some simple, convenient, and effective means of confidently eliminating the effects of several common condensed-phase chemical interferences.

Condensed-phase chemical interferences are classified as chemically specific interferences because their mechanism of origin purportedly rests in the formation of a thermally stable analyte-interferent chemical compound or matrix. Physical effects may also be manifested as apparent solute-vaporization interferences, and for this reason the observed interferences appear to be critically dependent on several experimental variables. An abundance of information suggests that the transformation of the sample aerosol into free analyte atoms in the flame is kinetically controlled. Therefore, the factors of primary importance that must be considered in the elimination of chemical interference effects are those that affect the rate of the aerosol desolvation and vaporization.

It is not possible to describe the behavior of the aerosol droplets at elevated flame temperatures by extrapolating from the equilibrium laws and solution chemistry. Insufficient information regarding the pyrochemistry of the aerosol in the flame prohibits a comprehensive analysis of the free-atom formation processes. However, certain factors are known to facilitate the vaporization of the desolvated aerosol and the production of the gaseous analyte. Experimentally, high temperature flames and a refinement of the sample aerosol have led to the mitigation of several chemical interference effects by increasing the rate of the aerosol vaporization process.

Recent developments in burner design and flame systems have provided the opportunity to exercise a higher degree of optimization in refining the aerosol reaching the flame and providing higher flame temperatures. This experimental study demonstrates that the solute-vaporization effects of phosphate and sulfate on the release of alkaline earth atoms in the flame can be virtually eliminated if the burner and flame systems described herein are employed. The alkaline earth-aluminum interferences, which are classified as solute-vaporization interferences, were also eliminated at interferent concentrations normally encountered by providing smaller aerosol particle size distributions and higher flame temperatures. However, the occurrence of ionization

interferences became increasingly important as the magnesium-, calcium-, strontium-, and barium-aluminum interferences were investigated in the N_2O-C_2H_2 slot burner flames. Ionization interferences can be eliminated by buffering the intrinsic ionization of the analyte with an excess of a salt such as KCl, which doesn't significantly affect the vaporization of the aerosol particle.

The increased importance of ionization in high temperature flames prompted an investigation of metal additive ionization in the nitrous oxide-acetylene flame. The purpose of this ionization study was to test the validity of Saha or equilibrium ionization of metal additives in a high temperature flame, which hitherto has not been employed for such a study. The plan of attack involved the evaluation of experimental ionization constants and a comparison of the observed ionization with equilibrium ionization.

Three experimental methods were devised to determine the experimental ionization constants; two of these methods also yielded values for the electron pressure in an unsalted flame. To determine the experimental ionization constants, absolute free-atom number densities were measured by the growth curves method and continuum absorption method and fractional ionizations of the metal vapor were measured by the ionization suppression technique.

Equilibrium ionization constants were calculated by applying the measured line reversal temperature to the Saha equation.

The observed ionization of calcium, strontium, sodium, and lithium deviated significantly from equilibrium ionization at various observation heights in the flame. These deviations were attributable to either slow ionization-recombination processes or chemi-processes or both.

The values derived for the electron pressure in an unsalted flame were in good agreement with results obtained in independent ionization investigations. The time-decay of the electron concentration in the unsalted flame was consistent with a second order recombination process. The rate constant of the recombination process was in good agreement with the published values for the rate constant in a fuel-rich flame.

LITERATURE CITED

1. Agarbiceanu, I., Kukurezianu, I., Popesku, I., and V. Vasiliu, Optics and Spectroscopy, 14, 8 (1963).

2. Alkemade, C. Th. J. A contribution to the development and understanding of flame photometry. Unpublished Ph.D. thesis. Utrecht, Holland, University of Utrecht. 1954.

3. Alkemade, C. Th. J., Anal. Chem., 38, 1252 (1966).

4. Alkemade, C. Th. J., Applied Optics, 7, 1261 (1968).

5. Alkemade, C. Th. J., in Tenth Colloquium Spectroscopicum Internationale, Lippincott, E. R. and M. Margoshes, Eds., Spartan Books, Washington, D. C., 1963, p 143.

6. Alkemade, C. Th. J., in Flame Emission and Atomic Absorption Spectrometry, Volume 1-Theory, Dean, J. A. and T. C. Rains, Eds., Marcel Dekker, Inc., New York, N.Y., 1969, Chapter 4.

7. Alkemade, C. Th. J. and M. E. J. Jeuken, Z. Anal. Chem., 158, 401 (1957).

8. Alkemade, C. Th. J. and M. H. Voorhuis, Z. Anal. Chem., 163, 91 (1958).

9. Allan, J. E., Analyst, 83, 466 (1958).

10. Amos, M. D. and J. B. Willis, Spectrochimica Acta, 22, 1325 (1966).

11. Baker, C. A. and F. W. J. Garton, A study of interferences in emission and absorption flame photometry, Atomic Energy Research Establishment Document AERE-R-3490, Harwell, U. K., 1961.

12. Baker, G. L. and L. H. Johnson, Anal. Chem., 26, 465 (1954).

13. Belcher, H. and T. M. Sugden, Proc. Roy. Soc., Ser. A, 201, 480 (1950).

14. Broida, H. P. and K. E. Shuler, J. Chem. Phys., 27, 933 (1957).

15. Bulewicz, E. M., Combustion and Flame, 11, 297 (1967).

16. Bulewicz, E. M., James, C. G., and T. M. Sugden, Proc. Roy. Soc., Ser. A, 235, 89 (1956).

17. Bulewicz, E. M. and P. J. Padley, Combustion and Flame, 5, 331 (1961).

18. Bulewicz, E. M. and P. J. Padley, Ninth Symposium (International) on Combustion, Academic Press, New York, N.Y., 1963, p 638.

19. Calcote, H. F., Combustion and Flame, 1, 385 (1957).

20. Calcote, H. F., Eighth Symposium (International) on Combustion, The Williams and Wilkins Co., Baltimore, Maryland, 1962, p 184.

21. Calcote, H. F., Ninth Symposium (International) on Combustion, Academic Press, New York, N.Y., 1963, p 622.

22. Calcote, H. F. in Progress in Astronautics and Aeronautics, Shuler, K. E. and J. B. Fenn, Eds., Academic Press, New York, N.Y., 1963, Vol. 12, p 107.

23. Calcote, H. F. and D. E. Jensen, Advances in Chemistry Series, No. 58, American Chemical Society, Washington, D. C., 1966, p 291.

24. Calcote, H. F. and I. R. King, Fifth Symposium (International) on Combustion, Reinhold Publishing Corporation, New York, N.Y., 1955, p 423.

25. Cowley, T. G., Fassel, V. A., and R. N. Kniseley, Spectrochimica Acta, 23B, 771 (1968).

26. David, D. J., Analyst, 84, 536 (1959).

27. David, D. J., Analyst, 85, 495 (1960).

28. Dean, J. A. and W. J. Carnes, Anal. Chem., 34, 192 (1962).

29. Deckers, J. and A. van Tiggelen, Combustion and Flame, 1, 281 (1957).

30. Deckers, J. and A. van Tiggelen, Seventh Symposium (International) on Combustion, Butterworths Scientific Publications, London, England, 1959, p 254.

31. de Galan, L., Smith, R., and J. D. Winefordner, Spectrochimica Acta, 23B, 521 (1968).

32. de Vos, J. C., Physica, 20, 690 (1954).

33. Dinnin, J. I., Anal. Chem., 32, 1475 (1960).

34. Dippel, W. A. A fundamental study of analytical flame photometry. Unpublished Ph.D. thesis. Princeton, New Jersey, Library, Princeton University. 1954.

35. Dippel, W. A., Bricker, C. E., and N. H. Furman, Anal. Chem., 26, 553 (1954).

36. Doty, M. E. Studies of suppression effects in emission flame photometry. Unpublished Ph.D. thesis. Manhattan, Kansas, Library, Kansas State University. 1963.

37. Douglas, B. E. and D. H. McDaniel, Concepts and Models of Inorganic Chemistry, Blaisdell Publishing Company, New York, N.Y., 1965.

38. Drawin, H. W. and P. Felenbok, Data for Plasmas in Local Thermodynamic Equilibrium, Gauthier-Villars, Paris, France, 1965.

39. D'Silva, A. P., Kniseley, R. N., and V. A. Fassel, Anal. Chem., 36, 1287 (1964).

40. Eisberg, R. M., Fundamentals of Modern Physics, John Wiley and Sons, Inc., New York, N.Y., 1961.

41. Electrical properties of flame---light, Scientific American, 7, 349 (1852).

42. Fassel, V. A., 18th Annual Mid-America Symposium on Spectroscopy, Chicago, Illinois, May 1967, No. 85.

43. Fassel, V. A. and D. A. Becker, in Thirteenth Colloquium Spectroscopicum Internationale, Adam Hilger Ltd., London, England, 1967, p 269.

44. Fenimore, C. P., The International Encyclopedia of Physical Chemistry and Chemical Physics, Topic 19-Gas Kinetics, A. F. Trotman-Dickenson, Ed., Pergamon Press, New York, N.Y., 1964.

45. Feugier, A. and A. van Tiggelen, Tenth Symposium (International) on Combustion, The Combustion Institute, Pittsburgh, Pennsylvania, 1965, p 621.

46. Fiorino, J. A., Kniseley, R. N., and V. A. Fassel, Spectrochimica Acta, 23B, 413 (1968).

47. Fristrom, R. M. and A. A. Westenberg, Flame Structure, McGraw-Hill Book Co., New York, N.Y., 1965.

48. Fukushima, S., Mikrochim. Acta, 596 (1959).

49. Gaydon, A. G., The Spectroscopy of Flames, Chapman and Hall Ltd., London, England, 1957.

50. Gaydon, A. G. and H. G. Wolfhard, Flames, Their Structure, Radiation and Temperature, 2nd edition, Chapman and Hall Ltd., London, England, 1960.

51. Gaydon, A. G. and H. G. Wolfhard, Proc. Roy. Soc., Ser. A, 205, 118 (1951).

52. Gilbert, P. T., Jr., Proceedings of the 10th National Analysis Instrumentation Symposium, Plenum Press, New York, N.Y., 1964, p 193.

53. Gould, E. S., Inorganic Reactions and Structure, Holt, Rinehart, and Winston, Inc., New York, N.Y., 1962.

54. Green, J. A. and T. M. Sugden, Ninth Symposium (International) on Combustion, Academic Press, New York, N.Y., 1963, p 607.

55. Gruzdev, P. F. and V. K. Prokofev, Optics and Spectroscopy, 21, 151 (1966).

56. Harrison, W. W. and W. H. Wadlin, Anal. Chem., 41, 374 (1969).

57. Hayhurst, A. N. and T. M. Sugden, Proc. Roy. Soc., Ser. A, 293, 36 (1965).

58. Hayhurst, A. N. and T. M. Sugden, Proc. Roy. Soc., Ser. A, 293, 136 (1965).

59. Hayhurst, A. N. and T. M. Sugden, Trans. Far. Soc., 63, 1375 (1967).

60. Heiftje, G. M. and H. V. Malmstadt, Anal. Chem., 40, 1860 (1968).

61. Herrmann, R., Alkemade, C. Th. J., and P. T. Gilbert, Jr., Chemical Analysis by Flame Photometry, 2nd revised edition, Interscience Publishers, New York, N.Y., 1963.

62. Herzberg, G., Atomic Spectra and Atomic Structure, 2nd edition, Dover Publications, Inc., New York, N.Y., 1944.

63. Hinnov, E., J. Opt. Soc. Am., 47, 151 (1957).

64. Hofmann, F. W. and H. Kohn, J. Opt. Soc. Am., 51, 512 (1961).

65. Hofmann, F. W., Kohn, H., and J. Schneider, J. Opt. Soc. Am., 51, 508 (1961).

66. Hollander, T., Amer. Inst. Aeronaut. Astronaut. J., 6, 385 (1968).

67. Hollander, T., Photometric measurements on the deviations from the equilibrium state in burnt flame gases, Advanced Research Projects Agency Technical Report No. 22, 1967.

68. Hollander, T. Self-absorption, ionization, and dissociation of metal vapour in flames. Unpublished Ph.D. thesis. Utrecht, Holland, University of Utrecht. 1964.

69. Hollander, T., Kalff, P. J., and C. Th. J. Alkemade, J. Chem. Phys., 39, 2558 (1963).

70. Homann, K. H. and H. G. Wagner, Eleventh Symposium (International) on Combustion, The Combustion Institute, Pittsburgh, Pennsylvania, 1967, p 371.

71. Hooymayers, H. P. Quenching of excited alkali atoms and hydroxyl radicals and related effects in flames. Unpublished Ph.D. thesis. Utrecht, Holland, University of Utrecht. 1966.

72. Ivanova, A. V. and A. N. Ivanova, Optics and Spectroscopy, 16, 499 (1964).

73. James, C. G. and T. M. Sugden, Nature, 171, 428 (1953).

74. James, C. G. and T. M. Sugden, Proc. Roy. Soc., Ser. A, 227, 312 (1955).

75. Jenkins, D. R. and T. M. Sugden, in Flame Emission and Atomic Absorption Spectrometry, Volume 1-Theory, Dean, J. A. and T. C. Rains, Eds., Marcel Dekker, Inc., New York, N.Y., 1969, Chapter 5.

76. Jensen, D. E. and P. J. Padley, Trans. Far. Soc., 62, 2140 (1966).

77. Kaskan, W. E., Combustion and Flame, 2, 229 (1958).

78. Kelly, R. and P. J. Padley, Trans. Far. Soc., 65, 355 (1969).

79. King, I. R., J. Chem. Phys., 31, 855 (1959).

80. King, I. R., J. Chem. Phys., 36, 553 (1962).

81. Knewstubb, P. F., Tenth Symposium (International) on Combustion, The Combustion Institute, Pittsburgh, Pennsylvania, 1965, p 623.

82. Knewstubb, P. F. and T. M. Sugden, Nature, 181, 474 (1958).

83. Knewstubb, P. F. and T. M. Sugden, Nature, 196, 1311 (1962).

84. Knewstubb, P. F. and T. M. Sugden, Proc. Roy. Soc., Ser. A, 255, 520 (1960).

85. Knewstubb, P. F. and T. M. Sugden, Seventh Symposium (International) on Combustion, Butterworths Scientific Publications, London, England, 1959, p 247.

86. Knewstubb, P. F. and T. M. Sugden, Trans. Far. Soc., 54, 372 (1958).

87. Leithe, W. and A. Hofer, Mikrochim. Acta, 168 (1961).

88. Lewis, B. and G. von Elbe, Combustion, Flames and Explosions of Gases, Academic Press, New York, N.Y., 1961.

89. Leyton, L., Analyst, 79, 497 (1954).

90. Manning, D. C. and L. Capacho-Delgado, Anal. Chim. Acta, 36, 312 (1966).

91. Margoshes, M. and B. L. Vallee, Anal. Chem., 28, 180 (1956).

92. Mavrodineanu, R. and H. Boiteux, Flame Spectroscopy, John Wiley and Sons, Inc., New York, N.Y., 1965.

93. Miller, W. J., Eleventh Symposium (International) on Combustion, The Combustion Institute, Pittsburgh, Pennsylvania, 1967, p 311.

94. Miller, W. J., Oxidation and Combustion Revs., 3, 97 (1968).

95. Mitchell, A. C. G. and M. W. Zemansky, Resonance Radiation and Excited Atoms, Cambridge University Press, New York, N.Y., 1934.

96. Mitchell, R. L., in Flame Emission and Atomic Absorption Spectrometry, Volume 1-Theory, Dean, J. A. and T. C. Rains, Eds., Marcel Dekker, Inc., New York, N.Y., 1969, Chapter 1.

97. Moore, W. J., Physical Chemistry, 3rd edition, Prentice-Hall, Inc., Englewood Cliffs, New Jersey, 1962.

98. Mossotti, V. and M. Duggan, Applied Optics, 7, 1325 (1968).

99. Myers, R. B., Kniseley, R. N., and V. A. Fassel, Pittsburgh Conference on Analytical Chemistry and Applied Spectroscopy, Pittsburgh, Pennsylvania, March 1967, No. 115.

100. Nesbitt, R. W., Anal. Chim. Acta, 35, 413 (1966).

101. Norrish, R. G. W., Tenth Symposium (International) on Combustion, The Combustion Institute, Pittsburgh, Pennsylvania, 1965, p 1.

102. Odintsov, A. I., Optics and Spectroscopy, 14, 172 (1963).

103. Olsen, H. N., Physics of Fluids, 3, 614 (1959).

104. Ostrovskii, Y. I. and N. P. Penkin, Optics and Spectroscopy, 11, 307 (1961).

105. Padley, P. J., Page, F. M., and T. M. Sugden, Trans. Far. Soc., 57, 1552 (1961).

106. Padley, P. J. and T. M. Sugden, Eighth Symposium (International) on Combustion, The Williams and Wilkins Co., Baltimore, Maryland, 1962, p 164.

107. Page, F. M. and T. M. Sugden, Trans. Far. Soc., 53, 1092 (1957).

108. Penkin, N. P. and L. N. Shabanova, Optics and Spectroscopy, 12, 1 (1962).

109. Penner, S. S., Quantitative Molecular Spectroscopy and Gas Emissivities, Addison-Wesley Publishing Company, Inc., Reading, Massachusetts, 1959.

110. Pickett, E. E. and S. R. Koirtyohann, Spectrochimica Acta, 23B, 235 (1968).

111. Poluektov, N. S. and M. P. Nikonova, Zhur, Anal. Khim., 13, 635 (1958).

112. Poncelet, J., Berendsen, R., and A. van Tiggelen, Seventh Symposium (International) on Combustion, Butterworths Scientific Publications, London, England, 1959, p 256.

113. Rains, T. C. in Flame Emission and Atomic Absorption Spectrometry, Volume 1-Theory, Dean, J. A. and T. C. Rains, Eds., Marcel Dekker, Inc., New York, N.Y., 1969, Chapter 12.

114. Rann, C. S., Spectrochimica Acta, 23B, 245 (1968).

115. Saha, M. N., Phil. Mag., 40, 472 (1920).

116. Schofield, K. and T. M. Sugden, Tenth Symposium (International) on Combustion, The Combustion Institute, Pittsburgh, Pennsylvania, 1965, p 589.

117. Schuhknecht, W. and H. Schinkel, Z. Anal. Chem., 143, 321 (1954).

118. Seshadri, K. S. and R. N. Jones, Spectrochimica Acta, 19, 1013 (1963).

119. Shuler, K. E. and J. Weber, J. Chem. Phys., 22, 491 (1954).

120. Slavin, W., Atomic Absorption Newsletter, 6, 9 (1967).

121. Smith, H. and T. M. Sugden, Proc. Roy. Soc., Ser. A, 211, 31 (1952).

122. Smith, H. and T. M. Sugden, Proc. Roy. Soc., Ser. A, 211, 58 (1952).

123. Smith, H. and T. M. Sugden, Proc. Roy. Soc., Ser. A, 219, 204 (1953).

124. Snelleman, W. A flame as a standard of temperature. Unpublished Ph.D. thesis. Utrecht, Holland, University of Utrecht. 1965.

125. Sugden, T. M., in Annual Review of Physical Chemistry, Eyring, H., Christensen, C. J., and H. S. Johnston, Eds., Annual Reviews, Inc., Palo Alto, California, 1962, Vol. 13, p 369.

126. Sugden, T. M., in Progress in Astronautics and Aeronautics, Shuler, K. E. and J. B. Fenn, Eds., Academic Press, New York, N.Y., 1963, Vol. 12, p 145.

127. Sugden, T. M., Tenth Symposium (International) on Combustion, The Combustion Institute, Pittsburgh, Pennsylvania, 1965, p 539.

128. Sugden, T. M. and P. F. Knewstubb, Research Correspondence, 9, S32 (1956).

129. Sugden, T. M. and R. C. Wheeler, Dis. Far. Soc., 19, 76 (1955).

130. van Tiggelen, A., in Progress in Astronautics and Aeronautics, Shuler, K. E. and J. B. Fenn, Eds., Academic Press, New York, N.Y., 1963, Vol. 12, p 165.

131. van Trigt, C., Hollander, T., and C. Th. J. Alkemade, J. Quant. Spectrosc. Radiat. Transfer, 5, 813 (1965).

132. West, A. C. Variables in flame spectrophotometry, their control and elimination. Unpublished Ph.D. thesis. Ithaca, New York, Library, Cornell University. 1961.

133. West, A. C. and W. D. Cooke, Anal. Chem., 32, 1471 (1960).

134. West, T. S., Analyst, 91, 69 (1966).

135. Willis, J. B., Spectrochimica Acta, 23A, 811 (1967).

136. Willis, J. B., Rasmuson, J. O., Kniseley, R. N., and V. A. Fassel. Spectrochimica Acta, 23B, 725 (1968).

137. Yofe, J. and R. Finkelstein, Anal. Chim. Acta, 19, 166 (1958).

138. Zeegers, P. J. T. Recombination of radicals and related effects in flames. Unpublished Ph.D. thesis. Utrecht, Holland, University of Utrecht. 1966.

139. Zeegers, P. J. T., Townsend, W. P., and J. D. Winefordner, Spectrochimica Acta, 24B, 243 (1969).

ACKNOWLEDGMENTS

I wish to gratefully acknowledge the guidance and assistance provided by Dr. Velmer A. Fassel during the seemingly endless course of this thesis research. Perhaps of greater importance was his gift of imbuing my mind with the virtues of patience, rapport, and timely acquiescence.

To Richard N. Kniseley I must express my personal thanks for his beneficial advice and gracious assistance that facilitated the completion of this thesis.

I'm also extremely appreciative for the understanding of my wife and my family: Scott, Chris, and number three, whoever that might be.